Design, Synthesis, and Lead Optimisation of CHVB Series Analogues as Potent Small Molecule Inhibitors of Chikungunya Virus

Verena Battisti,[*,†] Julia Moesslacher,[‡,⊥] Rana Abdelnabi,[¶] Pieter Leyssen,[¶] Ana Lucia Rosales Rosas,[¶] Lana Langendries,[¶] Mohammed Aufy,[§] Christian Studenik,[§] Jadel Kratz,[‖,#] Judith M. Rollinger,[‖] Gerhard Puerstinger,[‡] Johan Neyts,[¶] Leen Delang,[¶] Ernst Urban,[†] and Thierry Langer[*,†]

†*Department of Pharmaceutical Sciences, Pharmaceutical Chemistry Division, University of Vienna, Josef-Holaubek-Platz 2, A-1090 Vienna, Austria*

‡*Department of Pharmacy, University of Innsbruck, Innrain 80/82, A-6020 Innsbruck, Austria*

¶*Department of Microbiology, Immunology and Transplantation, Rega Institute for Medical Research, Laboratory of Virology and Chemotherapy, Herestraat 49, B-3000 Leuven, Belgium*

§*Department of Pharmaceutical Sciences, Division of Pharmacology and Toxicology, University of Vienna, Josef-Holaubek-Platz 2, A-1090 Vienna, Austria*

‖*Department of Pharmaceutical Sciences, Division of Pharmacognosy, University of Vienna, Josef-Holaubek-Platz 2, A-1090 Vienna, Austria*

⊥*Current address: CURA Marketing GmbH, Dr. Franz-Werner-Straße 19, A-6020 Innsbruck, Austria*

#*Drugs for Neglected Diseases initiative (DNDi), 1202 Geneva, Switzerland*

E-mail: verena.battisti@univie.ac.at; thierry.langer@unive.ac.at

Abstract

The worldwide re-emerge of the Chikungunya virus (CHIKV), the high morbidity associated with it, and the lack of an available vaccine or antiviral treatment make the development of a potent CHIKV-inhibitor highly desirable. Therefore, an extensive lead optimisation was performed based on the previously reported CHVB compound **1b** and the reported synthesis route was optimised - improving the overall yield in remarkable shorter synthesis and work-up time. 100 CHVB analogues were designed, synthesised, and investigated for their antiviral activity, physiochemistry, and toxicological profile. An extensive structure-activity relationship study (SAR) was performed, which focused mainly on the combination of scaffold changes and revealed the key chemical features for a high anti-CHIKV inhibition. Further, to investigate the druggability of the compound series, a thorough ADMET investigation was carried out: the compounds were screened for their aqueous solubility, lipophilicity, their toxicity in CaCo-2 cells, and possible hERG channel interactions. Additionally, 55 analogues were assessed for their metabolic stability in human liver microsomes (HLMs) which led to a structure-metabolism relationship study (SMR). The compounds showed an excellent safety profile, favourable physicochemical characteristics, and the required metabolic stability. A cross-resistance study confirmed the viral capping machinery (nsP1) to be the viral target of these second-generation CHVB compounds. This study identified five compounds (**31b**, **31d**, **32d**, **34**, and **35d**) as potent, safe, and stable lead compounds for further development as selective CHIKV inhibitors - with **32d** as the most promising candidate. Finally, the collected insight led to a successful scaffold hop (**64b**) for future antiviral research studies.

Introduction

Chikungunya virus (CHIKV) is a mosquito-borne alphavirus (*Togaviridae* family), first isolated from a febrile patient in 1952/53 in the Makonde plateau in Tanzania.[1] After only local and periodic outbreaks, a variant of CHIKV containing the A226V mutation in the E1

glycoprotein gene led to its re-emerging in 2004 on the coast of Kenya - marking the beginning of the successful CHIKV spreading worldwide.[2] This new CHIKV mutation changed the vector potential from primarily *Aedes aegypti* to the more global *Ae. albopictus* and thus enabling the virus to spread in new temperature zones.[3]

Consequently, since then, CHIKV outbreaks have been reported frequently in countries worldwide, causing millions of CHIKV infections every year.[4–7] Moreover, due to globalization, climate change, and lack of immunity in the worldwide population, this rapid spread of CHIKV is not only ongoing, but it is also reaching new territories and higher numbers of infections every year.[7–9]

Patients suffering from Chikungunya Fever (CHIKF) develop a high onset of fever for three to ten days, followed by a rash, myalgia, and nausea.[9] In addition, severe joint pain leads to the characteristic posture, which is also described in the Makonde word *Chikungunya* for "that which bends you up".[10] Moreover, approximately 50 % of CHIKF-patients develop chronic symptoms like severe arthralgia and myalgia persisting for months to years even after clearance of the acute viral infection.[11] Further, complications in vulnerable groups (e.g., patients with comorbidities, the elderly) have been reported.[12] Despite the severity and rapid spreading of CHIKV, there are no licensed drugs or vaccines available, and the alleviation of symptoms by, e.g. NSAIDs, remains the only possible treatment for CHIKF patients.[13,14] Therefore, developing safe and potent anti-CHIKV small molecules is highly desirable.

We previously reported a novel series N-ethyl-6-methyl-2-(4-(4-fluorophenylsulfonyl)piperazine-1-yl)pyrimidine-4-amine **1a** analogues with good biological activity against the CHIKV: the CHVB series. A structure-activity relationship (SAR) study was performed by dividing the compound into five groups. This led to the identification of the new lead compound **1b** (see **Figure 1**).[15,16]

However, although **1b** showed an improved *in vitro* anti-CHIKV activity and enhanced toxicological profile, these properties could still be improved, and additional assays of cru-

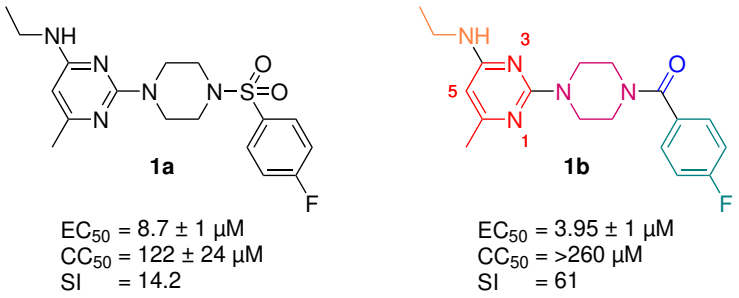

Figure 1. Structures of the first hit **1a** and the generated lead compound **1b** with their biological properties. The different colors of **1b** indicate the various groups of the CHVB series in which variations were performed and analyzed in the SAR studies. The described analogues were categorized according to their positioning of the nitrogens in the pyrimidine ring (P1/3, P3/5, and P1/5).

cial parameters in early drug design were missing. Therefore, a focused lead optimization based on the 2-(4-(phenylsulfonyl)piperazine-1-yl)pyrimidine scaffold was made to identify a CHVB analogue with enhanced antiviral activity, reduced toxicity, higher stability, and improved drug-like properties. For better accessibility of the designed analogues, an additional optimized synthesis route (Synthesis Route B) was established, and the overall 100 investigated analogues were categorized according to their positioning of the nitrogens in the pyrimidine ring (P1/3, P3/5, and P1/5).

Results and Discussion

Chemistry. **Scheme 1** depicts the established synthesis route (Synthesis Route A) for the synthesis of the 2-(4-phenylsulfonyl)piperazine-1-yl)pyrimidine analogues – also known as the CHVB series. The key intermediate **3a** was prepared via substitution reaction between 2,4-dichloro-6-methylpyrimidine **8a** and ethylamine and further reacted with tert-butyl-piperazine-1-carboxylate **2** under microwave conditions (**Scheme 2**). After deprotection of the piperazine, the desired compound **1b** was obtained via amidation.[15]

An easy and fast synthesis route was searched for the detailed investigation of the pyrimidine and ethylamine side chain. Therefore, Synthesis Route B was established, starting with the nucleophilic acyl substitution between the unprotected amino group of the Boc-protected

Scheme 1. Overview of possible synthesis routes for the lead compound 1b.[a]

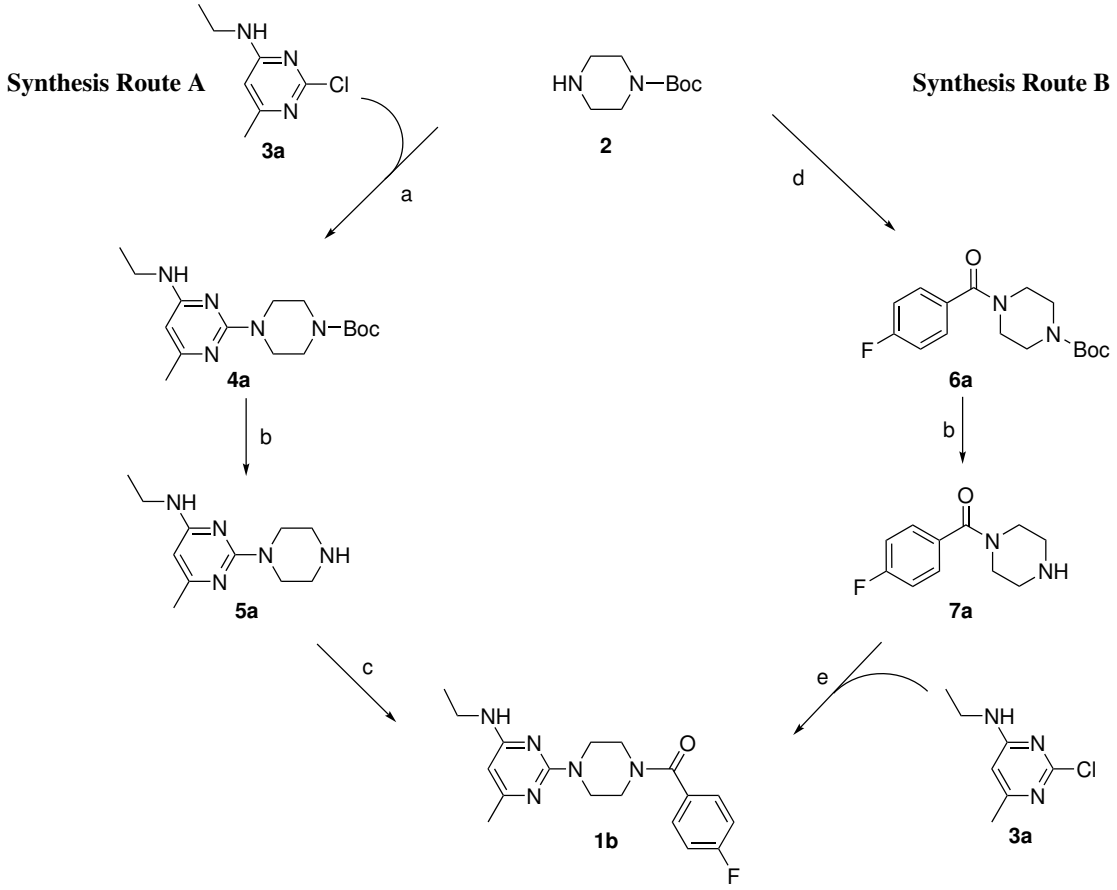

[a]Reagents and conditions: (a) EtOH, µwave, 30 min, 155 °C, 250 W, 12 bar (b) HCl/TFA, THF, 1 to 24 h, rt; (c) DCM, $N(CH_2CH_3)_3$, 24 h, rt, 4-fluorobenzenesulfonyl chloride; (d) pyridine, DMAP, 0 °C-rt, 15 h, 4-fluorobenzoyl chloride; (e) EtOH, DIPEA, µwave, 30 min, 155 °C, 250 W, 12 bar.

piperazine **2** and benzoyl chlorides. This reaction route enables synthesising significant variations on the desired pyrimidine and side-chain group of the compound series – as the modifications are introduced in the last and not the first step of the synthesis route. Furthermore, shortened reaction times, more accessible and sometimes unnecessary purification steps, and higher-yielding reactions lead to remarkable time- and yield-wise advantages to the published Synthesis Route A. Therefore, Synthesis Route B was subsequently used to synthesise all following analogues.

Synthesis Route B starts with a nucleophilic acyl substitution between Boc-protected piperazine and benzoyl chloride in pyridine with catalytic quantities of additional 4-dimethylaminopyridine (DMAP). The intermediate tert-butyl 4-(4-fluorobenzoyl)piperazine-

Scheme 2. Synthesis of the key intermediates 3a-h and 9a-h.[a]

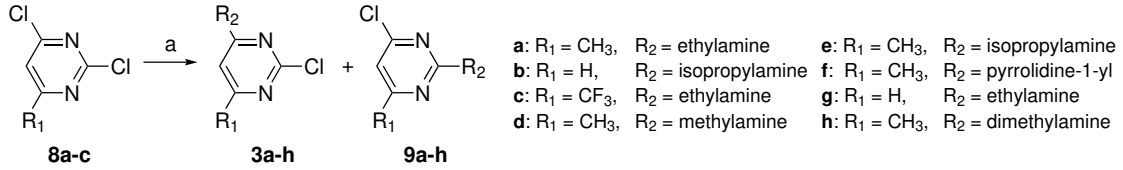

[a]Reagents and conditions: (a) Synthesis Route A: EtOH, 24 to 48 h, rt; Synthesis Route B: THF, 14 h, 0 °C-rt.

1-carboxylate **6a** precipitates in excellent yield while pouring the crude mixture on ice – facilitating the purification as the formed side products are water-soluble. Moreover, the following Boc-deprotection with trifluoroacetic acid (TFA) or hydrochloric acid (HCl) can also be performed without any purification step, which shortens the synthesis time by avoiding the time-consuming and challenging purification steps and increases the overall yield. This synthesis route's fourth and last step is the substitution reaction of the prepared arylamine **3a** and the de-protected piperazine intermediate **7a** under microwave irradiation in dry EtOH. The Hünig's base N,N-diisopropylethylamine (DIPEA), was introduced to this reaction as a proton scavenger. In addition, the solvent of the arylamine synthesis by amination of the commercially available 2,4-dichloropyrimidines shown in **Scheme 2** was changed from dry ethanol (EtOH) to dry Tetrahydrofuran (THF) – shifting the yield of 2-chloro-pyrimidin-4-amine **3a-h** to the much more desired 4-chloro-pyrimidin-2-amine **9a-h**.

Scheme 3 and **Scheme 4** outline the synthesis of 2-(piperazin-1-yl)pyrimidine **5a-d** and 4-(piperazin-1-yl)pyrimidine **21a-e** intermediates via Synthesis Route A. The reaction of these intermediates is essential for the synthesis of **1b** analogues - designed to carefully investigate the effects of various substitutions on both aromatic groups of an amide or sulfonamide bridge and their numerous combinations. The preparation of **2** was carried out similar to the published procedure of Moussa et al..[17]

13 was synthesized directly from the purchased 2-(piperazin-1-yl)pyrimidine **5e** and 4-fluorobenzenesulfonyl chloride in one step. To investigate the importance of a carbonyl- or sulfonyl-linker, analogue **23** with a methyl-4-fluorobenzene group was synthesized via Synthesis Route A using 1-(chloromethyl)-4-fluorobenzene. Similarly, to explore the precise

Scheme 3. Synthesis Route A for synthesis of compounds with a P1/3 pyrimidine nitrogen position (10a-19).[a]

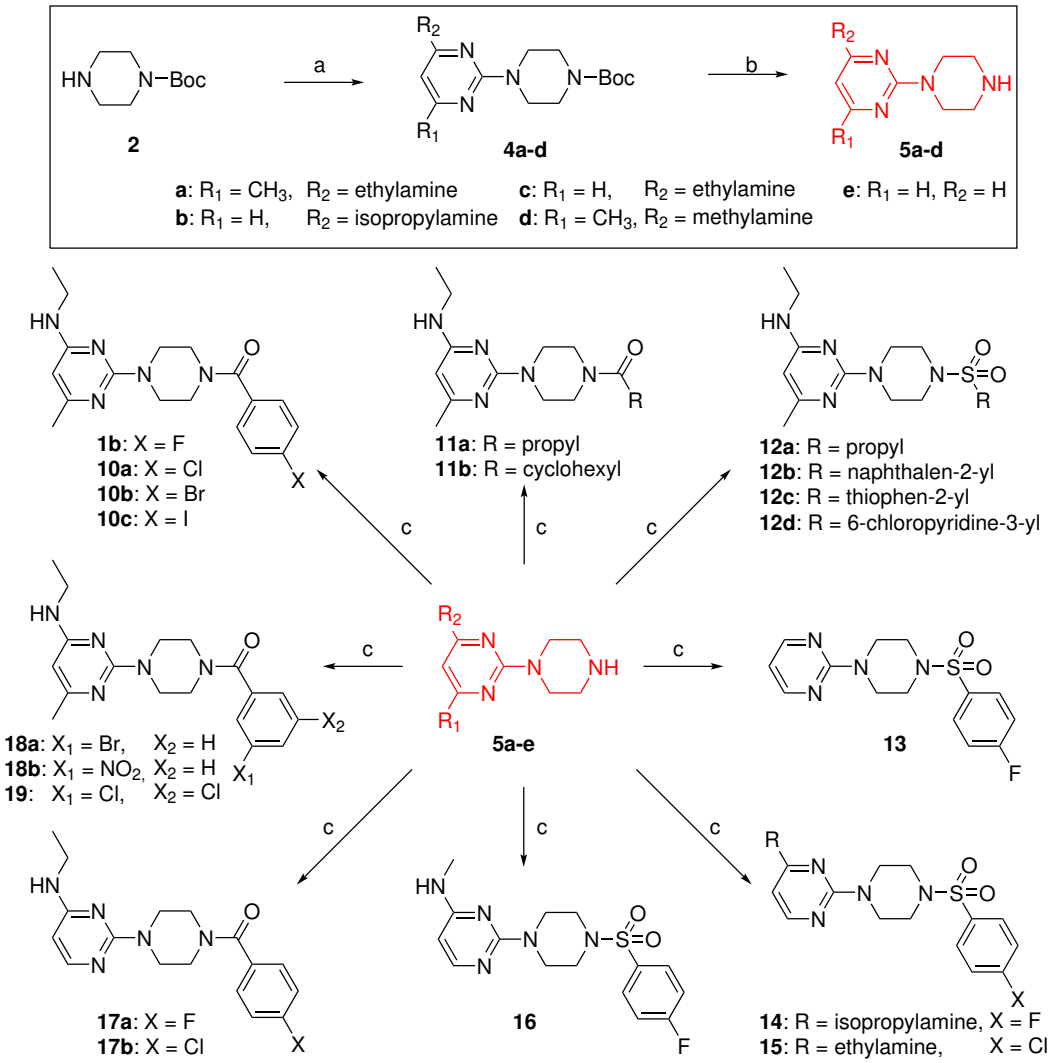

[a]Reagents and conditions: (a) EtOH, µwave, 30 min, 155 °C, 250 W, 12 bar, **8a**; (b) HCl, THF, 24 h, rt; (c) DCM, $N(CH_2CH_3)_3$, 24 h, rt, benzenesulfonyl chloride/benzoyl chloride. Key intermediates **4a-d** are highlighted in red.

role of the nitrogens and their position in the pyrimidine ring analogue N-ethyl-6-(4-((4-fluorophenyl)sulfonyl)piperazin-1-yl)pyrimidin-4-amine **39** was prepared to deploy the same reaction conditions from Synthesis Route A with 6-chloro-N-ethylpyrimidin-4-amine **36** (see Supporting Information, **Scheme S1**).

Scheme 5 depicts the synthesis of pyrimidine and side-chain analogues of our compound series using the versatile Synthesis Route B. The acylation of the Boc-protected piperazine with neat benzoyl chlorides to form monosubstituted amide products **6a-f** was carried out

Scheme 4. Synthesis Route A for synthesis of compounds with a P3/5 pyrimidine nitrogen position (22-35d).[a]

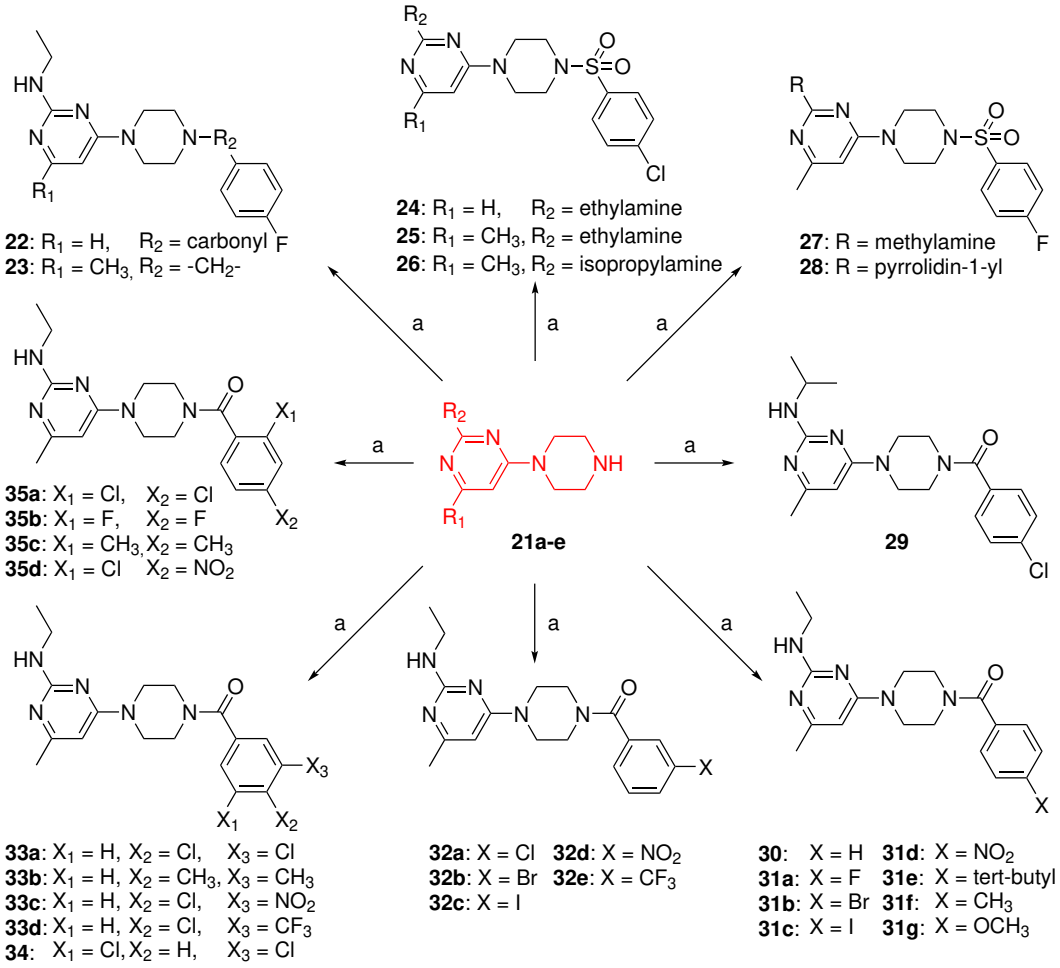

[a]Reagents and conditions: (a) DCM, $N(CH_2CH_3)_3$, 24 h, rt, benzenesulfonyl chloride/benzoyl chloride/1-(chloromethyl)-4-fluorobenzene. Key intermediates **21a-e** are shown in red.

in pyridine under basic conditions. DMAP was employed as a strong nucleophilic catalyst. After deprotection of the piperazine-nitrogen, the coupling of the aryl halide (**3a-h**, **9a-h**) with the secondary amine of **7a-f** was performed under microwave irradiation (250 W) and pressure (12 bar) for 30 min while heated to 100 °C.

The synthesis of the intermediate **51**, which is used to form the analogues **52a** and **52b**, is shown in **Scheme 6**. Commercially available 5-amino-4,6-dichloro-2-methylpyrimidine

Scheme 5. Synthesis Route B for synthesis of pyrimidine and side-chain analogues (40a-48).[a]

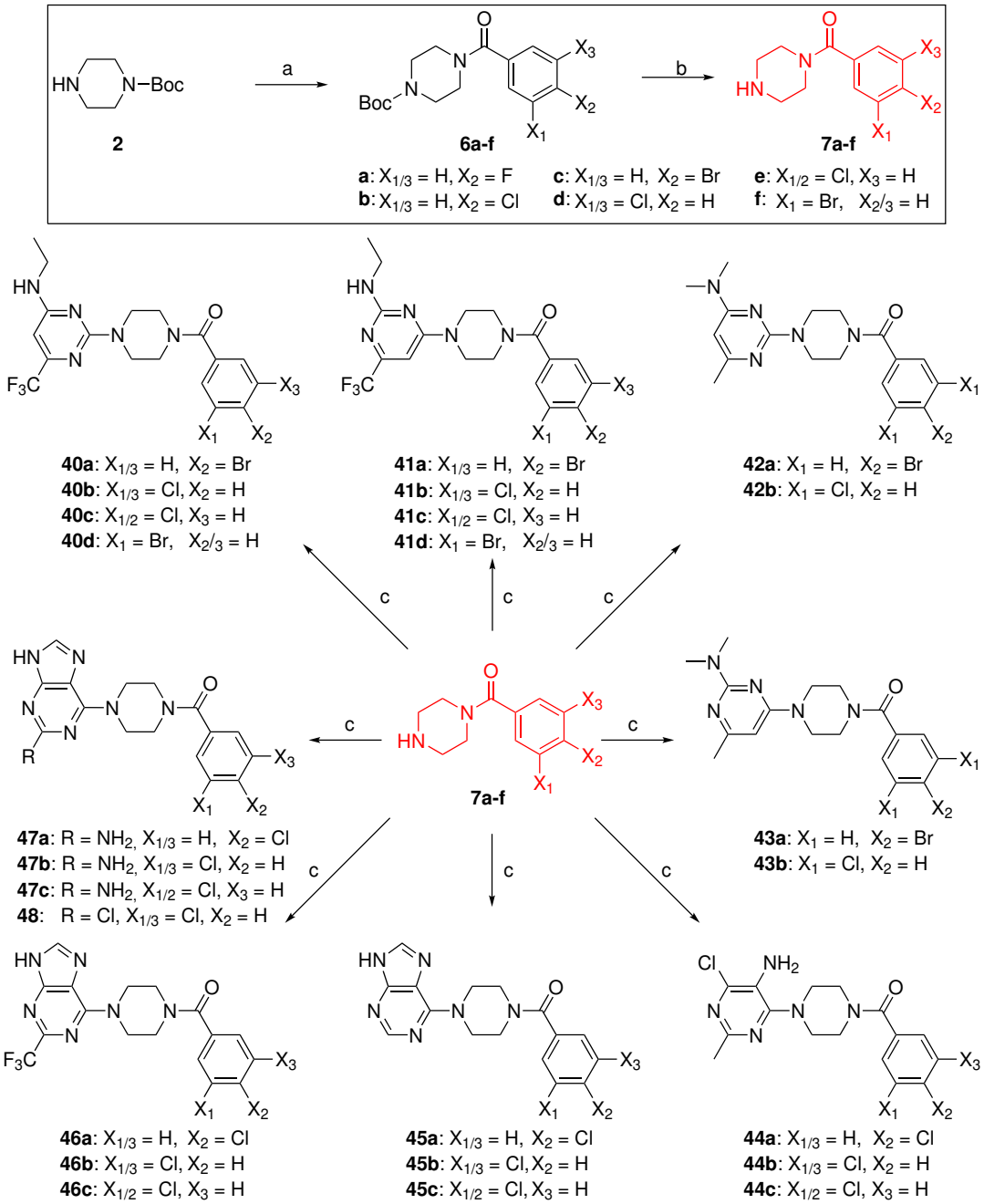

[a]Reagents and conditions: (a) pyridine, DMAP, 0 °C-rt, 15 h, benzoyl chloride; (b) TFA, THF, 1 to 15 h, rt; (c) EtOH, DIPEA, μwave, 30 min, 155 °C, 250 W, 12 bar, aryl halide. Key intermediates **6a-f** are highlighted in red.

Scheme 6. Synthesis of compound (52a-b).[a]

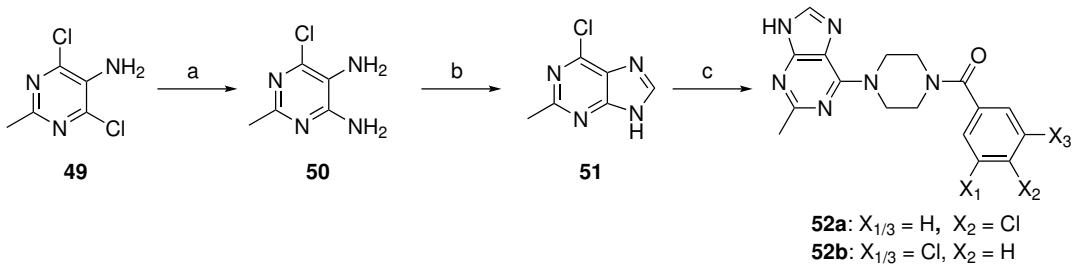

[a]Reagents and conditions: (a) conc. NH_3, 120 °C, 24 h; (b) TEOF, FA, 5.5 h, 120 °C; (c) EtOH, DIPEA, µwave, 30 min, 155 °C, 250 W, 12 bar.

---

49 was converted to 4,5-diamino-6-chloro-2-methyl-pyrimidine **50** via amination of the aryl halide with concentrated NH_3 at 120 °C.[18] Treatment with formic acid (FA) and triethyl orthoformate (TOFA) afforded the intermediate **51** via Traube purine synthesis.[18]

To investigate the importance of the piperazine and to confirm the previous results published earlier, which indicate that the piperazine functions solely as a linker between the two more critical aromatic parts of the compound series, a set of piperazine-analogues was designed and synthesized applying Synthesis Route B (**Scheme 7**). Similarly, the reaction between the commercially available spiro[chromane-2,4'-piperidin]-4-one **63** and the pyrimidine intermediates **3a** and **9a** afforded **64a** and **64b**, respectively (**Scheme 8**).

Structure-Activity Relationship Study. This structure-activity relationship (SAR) study focused mainly on the combination of scaffold changes. All 100 final compounds were evaluated for their inhibitory activity against the Chikungunya virus via virus cell-based CPE reduction assay in Vero cells, and their results are summarised in **Table 1-5**. As stated by Moesslacher et al., the nitrogen positions on the pyrimidine ring can positively impact the antiviral activity.[15] From all studied nitrogen positions on the pyrimidine ring, the position P3/5 gave the best antiviral result ($EC_{50} = 3.2 \pm 0.2\,\mu M$). Surprisingly, when combined with other alterations, the activity got lost.[15] To further investigate these unexpected results and to find a combination of the promising nitrogen positions, 100 P1/3,

Scheme 7. Synthesis Route B for the synthesis of piperazine analogues (55a-62d).[a]

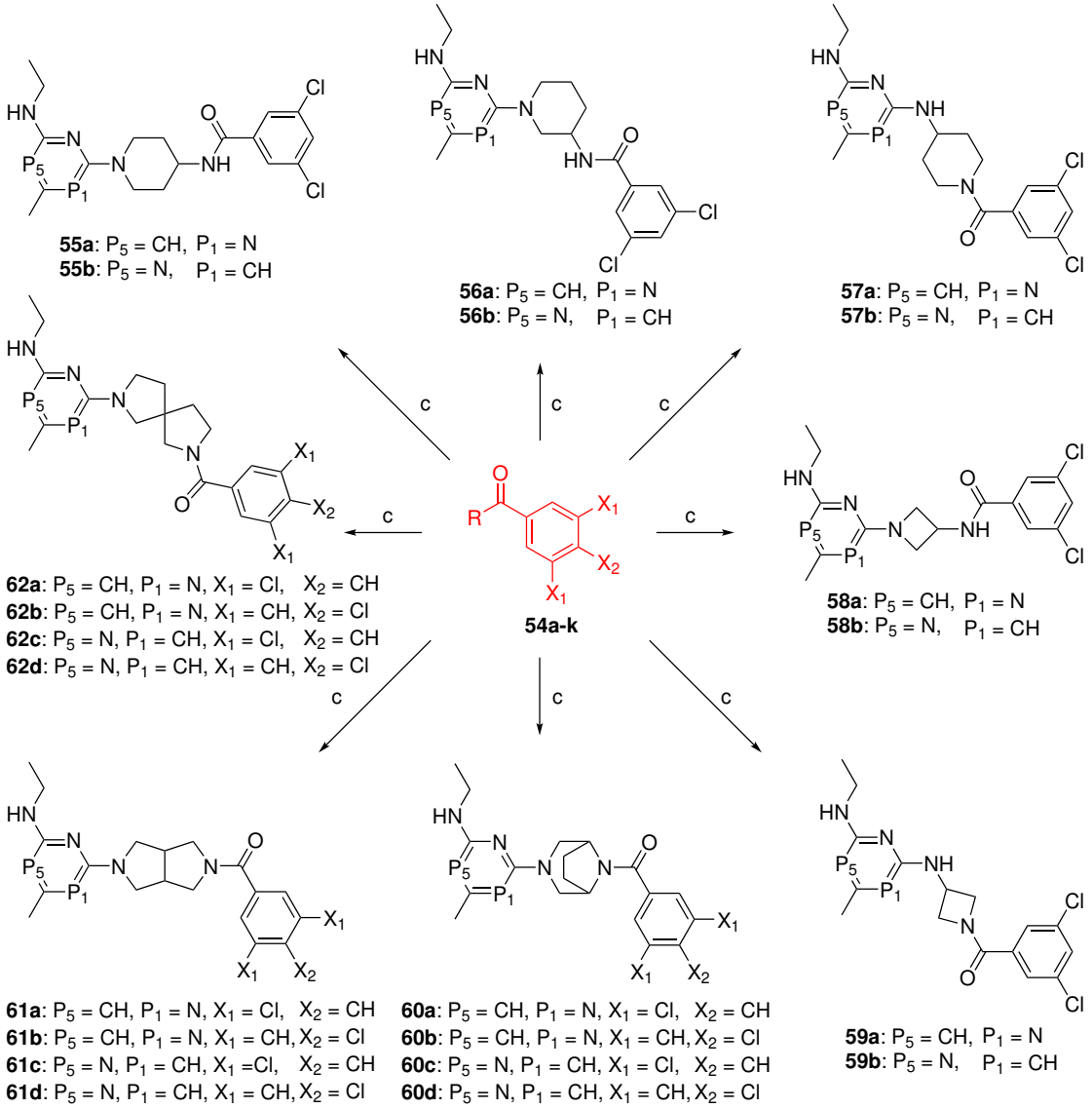

[a]Reagents and conditions: (a) EtOH, DIPEA, µwave, 30 min, 155 °C, 250 W, 12 bar, aryl halide. Key intermediates **54a-k** are highlighted in red and are synthesized according to Synthesis Route B.

P3/5 and P1/ 5 analogues were analyzed – focusing on different alterations alone and in combination (with/without/substituted methyl group; ethylamine/smaller or larger sidechains; sulfonamide/amide/methylene; various phenyl-substitutions on different positions).

Pyrimidine Nitrogen Position 1/3 Scaffold. First, the impact of various functional groups was investigated by replacing them with different classical and non-classical bioisosteres and by testing analogues without them. Therefore, the influence of the phenyl

Scheme 8. Synthesis of compound (64a-b).[a]

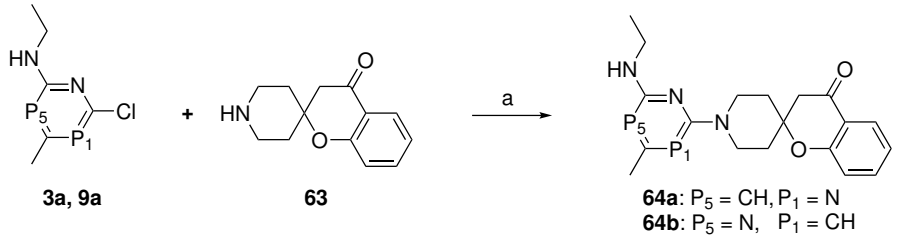

[a]Reagents and conditions: (a) EtOH, DIPEA, µwave, 30 min, 155 °C, 250 W, 12 bar.

Table 1. Antiviral activity and ADME properties of sulfonamide analogues 12a-16 (P1/3 scaffold) and with 23-28 (P3/5 scaffold).[a]

Compounds[b]	EC_{50} (µM)[f]	CC_{50} (µM)[g]	SI[h]	Half-Life (min)[i]	Aq. Sol. (pH 7.4; µM)[j]	$cLogD_{pH\ 7.4}$[k]
12a[c]	70 ± 18	n.d.	n.d.		>120	2.93
12b[c]	10 ± 0.4	17 ± 3.8	1.7	20 ± 0.6	90 ± 22	3.53
12c[c]	103	180	1.8		68 ± 11.5	3.11
12d[c]	121	97	0.8		115 ± 1.1	2.81
13[c]	310	n.d.	n.d.		64 ± 14	2.40
14[c]	10 ± 1.2	n.d.	n.d.	46 ± 1.2	100 ± 13	3.41
15[c]	10 ± 3.1	28 ± 23	2.7	19 ± 0.78	94 ± 37	3.33
16[c]	9.6 ± 0.23	193 ± 11	20	48 ± 4.5	>120	3.02
23[c,d]	22 ± 24	46 ± 47	2.1	78 ± 5.5	106 ± 15	3.35
24[e]	16 ± 3.7	44 ± 6.6	2.7	62 ± 8.6	95 ± 5	3.33
25[e]	2.8	11 ± 3.1	3.9	49 ± 2.6	104 ± 22	3.44
26[e]	3.8 ± 1.07	19 ± 4.2	4.9	54 ± 3.5	76 ± 15	3.62
27[e]	11 ± 0.94	99 ± 35	9.2	226 ± 13	>120	2.93
28[e]	25 ± 7	47 ± 21	1.9		>120	3.44

(a) Data represent mean values ± SD from at least three independent experiments. ND - not detectable. (b) Compounds synthesized according to Synthesis Route A. (c) Compounds with a P1/3 scaffold. (d) Compound with a methylene scaffold. (e) Compounds with a P3/5 scaffold. (f) The 50 % effective concentration (EC_{50}) is the concentration of compound that is required to inhibit virus-induced cell death by 50 %. (g) The 50 % cytostatic/cytotoxic concentration (CC_{50}) is the concentration of compound that reduces the overall metabolic activity of the uninfected, compound-treated cells by 50 % as compared to the untreated, uninfected cell. (h) The selectivity index (SI) is the ration between CC_{50} and EC_{50}. (i) The half-life (min) in human liver microsomes with 60 min incubation is estimated from the slope of the initial linear range of the logarithmic curve of compound remaining (%) vs time, assuming the first-order kinetics. (j) The aqueous solubility ($pH_{7.4}$) is measured by HPLC and calculated by the AUC (Absorbance Unit under the Curve) values of the buffered samples divided by the AUC values of the control samples. (k) clogD is calculated by the Graph Neural Network D-GIN [19]

was examined with different aliphatic and (hetero)aromatic replacements (**11a-b** and **12a-d**) in combination with an amide or sulfonamide linker. None of the tested analogues showed any antiviral activity (see **Table 1-2**). Similar, **13** - missing the ethylamine and the methyl group on the pyrimidine ring - showed no antiviral activity at all - underlying the importance of the two aliphatic groups on the pyrimidine ring.

To further explore the impact of the methyl group, various analogues with scaffold modifications combined with a missing methyl group were designed and tested for antiviral activity. Neither of these analogues gave any advantage on the viral activity (**15** and **17a-b**). In-

Table 2. Antiviral activity and ADME properties of P1/3 nitrogen and amide scaffold analogues.[a]

Compounds	EC_{50} (µM)[d]	CC_{50} (µM)[e]	SI[f]	Half-Life (min)[g]	Aq. Sol. (pH 7.4 µM)[h]	$cLogD_{pH\ 7.4}$[i]
10a[b]	2.4	89 ± 10	37	148 ± 13	>120	3.30
10b[b]	9.6	>100	10	91 ± 2.2	116 ± 6	3.25
10c[b]	2.9	>100	34	76 ± 3.8	116 ± 2.8	2.91
11a[b]	67	n.d.	n.d.		>120	2.64
11b[b]	70 ± 6	147 ± 61	2.1		119 ± 1	3.30
17a[b]	3.9 ± 1.5	183 ± 42	47	328 ± 6	>120	3.01
17b[b]	15 ± 3.7	47 ± 24	3.1	137 ± 25	>120	3.19
18a[b]	5.1 ± 1.7	>100	20	9.5 ± 0.57	>120	3.28
18b[b]	4.2 ± 1.9	>100	24	57 ± 1.5	119 ± 1.20	2.87
19[b]	67	>100	1.5		11	3.52
40a[c]	>6.3	>25	4	56 ± 3	1.2	3.66
40b[c]	>6.3	>25	4	18 ± 1.2	3.5	3.81
40c[c]	>6.3	>25	4	36 ± 0.7	0	3.80
40d[c]	41 ± 19	n.d.	n.d.	17 ± 1.2	0.80	3.68
42a[c]	13	76	6.02	29 ± 1.5	114 ± 8.6	3.28
42b[c]	>100	>100	1		95 ± 1.4	3.51

(a) Data represent mean values ± SD from at least three independent experiments. ND - not detectable. (b) Compounds synthesized according to Synthesis Route A. (c) Compounds synthesized according to Synthesis Route B. (d) The 50 % effective concentration (EC_{50}) is the concentration of compound that is required to inhibit virus-induced cell death by 50 %. (e) The 50 % cytostatic/cytotoxic concentration (CC_{50}) is the concentration of compound that reduces the overall metabolic activity of the uninfected, compound-treated cells by 50 % as compared to the untreated, uninfected cell. (f) The selectivity index (SI) is the ration between CC_{50} and EC_{50}. (g) The half-life (min) in human liver microsomes with 60 min incubation is estimated from the slope of the initial linear range of the logarithmic curve of compound remaining (%) vs time, assuming the first-order kinetics. (h) The aqueous solubility ($pH_{7.4}$) is measured by HPLC and calculated by the AUC (Absorbance Unit under the Curve) values of the buffered samples divided by the AUC values of the control samples. (i) clogD is calculated by the Graph Neural Network D-GIN [19]

terestingly, combined with the bigger and flexible side chain isopropylamine, the missing methyl group in **14** had no impact on the antiviral activity (EC_{50} = 10.6 µM). Moreover, the shortened methylamine side-chain gave a similar good antiviral activity (**16**, EC_{50} = 9.62 µM, see **Table 1-2**).

In addition, other substitution patterns and different rests on the phenyl were tested for their antiviral impact. Therefore, **10a-c** with different halogen substitutions on the para position were synthesized. The chloride and iodide substitution showed good antiviral activity (EC_{50} of 2.4 and 2.9 µM), whereas the bromide analogue **10b** remained active but with a declined activity (EC_{50} = 9.58 µM). Interestingly, the shift of the bromide from the para to the meta position in **18a** improved the antiviral activity to an EC_{50} value of 5.11 µM. On the other hand, the di-para halogen substituted analogue **19** showed no antiviral activity (see **Table 2**).

Pyrimidine Nitrogen Position 3/5 Scaffold. The biological data of the compounds bearing a P3/5 scaffold is shown in **Table 1**, **3**, and **5**. First, the impact of the methyl

Table 3. Antiviral activity and ADME properties of P3/5 nitrogen and amide scaffold analogues.[a]

Compounds	EC_{50} (µM)[d]	CC_{50} (µM)[e]	SI[f]	Half-Life (min)[g]	Aq. Sol. (pH 7.4 µg)[h]	$cLogD_{pH\ 7.4}$[i]
22[b]	216 ± 7.1	>304	1.4		>120	2.99
29[b]	18 ± 5.4	46 ± 15	2.6	176 ± 30	115 ± 6.5	3.43
30[b]	2.05 ± 1.1	>308	150	329 ± 119	>120	2.43
31a[b]	1.5 ± 0.84	165 ± 28	109	388 ± 5	>120	3.00
31b[b]	0.6 ± 0.08	>96	159	192 ± 28	>120	3.22
31c[b]	0.7 ± 0.28	58 ± 17	82	148 ± 2	112 ± 11	2.84
31d[b]	0.91 ± 0.18	>100	110	3536 ± 528	>120	2.81
31e[b]	2.4 ± 0.45	45	19	92 ± 7	120 ± 0.28	3.81
31f[b]	2.4 ± 0.25	203 ± 79	84	458 ± 195	>120	3.21
31g[b]	1.4 ± 0.07	136 ± 130	97	584 ± 77	>120	2.70
32a[b]	6.6 ± 0.79	248	38	93 ± 5	>120	3.29
32b[b]	0.94 ± 0.03	>100	107	74 ± 2	>120	3.25
32c[b]	1	>100	98	42 ± 3	>120	2.89
32d[b]	0.7 ± 0.05	>100	143	391 ± 140	>120	2.83
32e[b]	1.3 ± 0.18	80	60	91 ± 19	>120	3.51
33a[b]	0.57	46 ± 12	81	94 ± 9.4	111 ± 12.8	3.51
33b[b]	0.95 ± 0.46	65	68	123 ± 35	118 ± 2.6	3.42
33c[b]	0.98 ± 0.06	>20	20	187 ± 24	>120	3.07
33d[b]	1.9 ± 0.41	>20	11	75 ± 17	101 ± 12	3.69
34[b]	0.47 ± 0.06	80	173	90 ± 18	108 ± 17	3.49
35a[b]	>100	47	0.47		>120	3.38
35b[b]	>100	>100	>1		n.d.	2.92
35c[b]	>100	>100	>1		n.d.	2.93
35d[b]	>0.78	>100	128	204 ± 4	111 ± 13	3.09
41a[c]	>100	>100	1		33 ± 1.6	3.66
41b[c]	>12.5	>50	4	29 ± 1.6	2 ± 1.7	3.83
41c[c]	>100	>100	1		0	3.83
41d[c]	100	>100	1		n.d.	3.78
43a[c]	6.6	>100	15	108 ± 14	>120	3.28
43b[c]	4.4	67	15	108 ± 1.1	109 ± 2.1	3.51

(a) Data represent mean values ± SD from at least three independent experiments. ND - not detectable. (b) Compounds synthesized according to Synthesis Route A. (c) Compounds synthesized according to Synthesis Route B. (d) The 50 % effective concentration (EC_{50}) is the concentration of compound that is required to inhibit virus-induced cell death by 50 %. (e) The 50 % cytostatic/cytotoxic concentration (CC_{50}) is the concentration of compound that reduces the overall metabolic activity of the uninfected, compound-treated cells by 50 % as compared to the untreated, uninfected cell. (f) The selectivity index (SI) is the ration between CC_{50} and EC_{50}. (g) The half-life (min) in human liver microsomes with 60 min incubation is estimated from the slope of the initial linear range of the logarithmic curve of compound remaining (%) vs time, assuming the first-order kinetics. (h) The aqueous solubility ($pH_{7.4}$) is measured by HPLC and calculated by the AUC (Absorbance Unit under the Curve) values of the buffered samples divided by the AUC values of the control samples. (i) clogD is calculated by the Graph Neural Network D-GIN [19]

group regarding the anti-CHIKV-activity was investigated. Therefore, compounds without the methyl group and the P3/5 variation were designed and subsequently compared with the corresponding methylated analogues for their biological activity. In line with the results discussed above, all the un-methylated compounds showed a much higher EC_{50} value (**24** with EC_{50} = 15.9 µM vs. **25** with EC_{50} = 2.76 µM) or even a loss of activity (**22** with EC_{50} = 216 µM vs. **31a** with EC_{50} = 1.52 µM). Interestingly, compared to the corresponding

Table 4. Antiviral activity and ADME properties of P1/5 nitrogen and/or purine scaffold analogues.[a]

Compounds[b]	EC_{50} (µM)[c]	CC_{50} (µM)[d]	SI[e]	Half-Life (min)[f]	Aq. Sol. (pH 7.4 µg)[g]	$cLogD_{pH\ 7.4}$[h]
39	>274	n.d.	n.d.		94 ± 12	3.20
44a	>88	>88	>1		n.d.	2.41
44b	32 ± 0.7	n.d.	n.d.		94 ± 8	3.16
44c	9.8 ± 0.35	n.d.	n.d.	128 ± 3.3	118 ± 3	3.15
45a	94 ± 2	n.d.	n.d.		114 ± 5	2.60
45b	32 ± 3.7	n.d.	n.d.		112 ± 0.4	3.17
45c	66 ± 6.5	n.d.	n.d.		104 ± 13	3.00
46a	26 ± 0.06	n.d.	n.d.		36 ± 2.1	3.39
46b	77	n.d.	n.d.		73 ± 16	3.55
46c	9.5 ± 0.39	n.d.	n.d.	120 ± 16	71 ± 13	3.44
47a	>100	n.d.	n.d.		116 ± 3.7	2.56
47b	>100	n.d.	n.d.		47 ± 12	2.81
47c	>100	n.d.	n.d.		106 ± 17	2.71
48	18 ± 2.8	n.d.	n.d.	142 ± 1.8	66 ± 6.5	3.30
52a	97 ± 0.47	n.d.	n.d.		84 ± 51	2.56
52b	>100	n.d.	n.d.		92 ± 22	3.21

(a) Data represent mean values ± SD from at least three independent experiments. ND - not detectable. (b) Compounds synthesized according to Synthesis Route B. (c) The 50 % effective concentration (EC_{50}) is the concentration of compound that is required to inhibit virus-induced cell death by 50 %. (d) The 50 % cytostatic/cytotoxic concentration (CC_{50}) is the concentration of compound that reduces the overall metabolic activity of the uninfected, compound-treated cells by 50 % as compared to the untreated, uninfected cell. (e) The selectivity index (SI) is the ration between CC_{50} and EC_{50}. (f) The half-life (min) in human liver microsomes with 60 min incubation is estimated from the slope of the initial linear range of the logarithmic curve of compound remaining (%) vs time, assuming the first-order kinetics. (g) The aqueous solubility ($pH_{7.4}$) is measured by HPLC and calculated by the AUC (Absorbance Unit under the Curve) values of the buffered samples divided by the AUC values of the control samples. (h) clogD is calculated by the Graph Neural Network D-GIN [19]

analogue **17a** with the pyrimidine nitrogen pattern P1/3 and an EC_{50} value of 3.89 µM, the missing methyl group had a much greater impact on the inactive **22** – indicating that the P3/5 nitrogen position is much more sensitive to the presence of the methyl group. Further, also the nitrogen position P1/5 seems to be affected by the missing methyl group as **39** demonstrated no antiviral activity.

Notably, analogues bearing a CF_3 with a similar size but higher lipophilicity than the replaced methylgroup exhibit low activity (**41a-d**) - whereas in the case of P1/3 pyrimidine analogues, no activity was observed (**40a-c**; except of **40d** with weak antiviral activity of $EC_{50} = 40.95 \pm 19.33$ µM).

Subsequently, different ethylamine replacements were tested to investigate the requirements (i.e., lipophilic, H-bonding, or steric requirements/limitations) for antiviral activity combined with the P3/5 nitrogen shift. Two analogues with various lengths and steric requirements were prepared and evaluated to examine the influence of different steric sizes (**Table 1** and **3**). The bulkier and more rigid pyrrolidine replacement **28** showed almost

Table 5. Antiviral activity and ADME properties of piperazine bioisostere scaffold analogues.[a]

Compounds[b]	EC_{50} (µM)[e]	CC_{50} (µM)[f]	SI[g]	Half-Life (min)[h]	Aq. Sol. (pH 7.4 µg)[i]	$cLogD_{pH\ 7.4}$[j]
55a[c]	>100	48	0.48		52 ± 29	3.56
55b[d]	>25	>100	4		100 ± 28	3.53
56a[c]	>25	49	1.95		31 ± 26	3.59
56b[d]	>100	12	0.12	44 ± 0.28	22 ± 1.6	3.57
57a[c]	12	25	2.02	30 ± 0.71	94 ± 3	3.15
57b[d]	14	47	3.4	78 ± 10	101 ± 2.6	3.17
58a[c]	>88	n.d.	n.d.		47 ± 7.6	3.28
58b[d]	>100	n.d.	n.d.		81 ± 0.92	3.27
59a[c]	>100	n.d.	n.d.		93 ± 1.6	3.30
59b[d]	8.5 ± 0.52	n.d.	n.d.	37 ± 1.8	104 ± 5	3.30
60a[c]	>100	n.d.	n.d.		97 ± 19	3.45
60b[c]	79 ± 14	>88	1.11		n.d.	3.21
60c[d]	14 ± 1.9	n.d.	n.d.	85 ± 0.57	111 ± 13	3.42
60d[d]	17 ± 3.4	84 ± 9.9	5		n.d.	3.19
61a[c]	23 ± 1.9	n.d.	n.d.		108 ± 15	3.34
61b[c]	12 ± 1.3	>88	7.5		n.d.	3.09
61c[d]	19 ± 1.7	n.d.	n.d.	64 ± 6.2	109 ± 5.1	3.35
61d[d]	3.2 ± 0.28	72 ± 6	23		n.d.	3.09
62a[c]	28 ± 1.5	n.d.	n.d.		108 ± 18	3.42
62b[c]	32 ± 3.8	74	2.3		n.d.	3.17
62c[d]	11 ± 0.33	n.d.	n.d.	74 ± 12	98 ± 3	3.40
62d[d]	18 ± 2.1	45 ± 1.7	2.5		n.d.	3.17
64a[c]	23 ± 4	n.d.	n.d.		100 ± 3	2.61
64b[d]	4.2 ± 0.15	n.d.	n.d.	91 ± 5	98 ± 8	2.49

(a) Data represent mean values ± SD from at least three independent experiments. ND - not detectable. (b) Compounds synthesized according to Synthesis Route B. (c) Compounds with a P1/3 scaffold. (d) Compounds with a P3/5 scaffold. (e) The 50 % effective concentration (EC_{50}) is the concentration of compound that is required to inhibit virus-induced cell death by 50 %. (f) The 50 % cytostatic/cytotoxic concentration (CC_{50}) is the concentration of compound that reduces the overall metabolic activity of the uninfected, compound-treated cells by 50 % as compared to the untreated, uninfected cell. (g) The selectivity index (SI) is the ration between CC_{50} and EC_{50}. (h) The half-life (min) in human liver microsomes with 60 min incubation is estimated from the slope of the initial linear range of the logarithmic curve of compound remaining (%) vs time, assuming the first-order kinetics. (i) The aqueous solubility ($pH_{7.4}$) is measured by HPLC and calculated by the AUC (Absorbance Unit under the Curve) values of the buffered samples divided by the AUC values of the control samples. (j) clogD is calculated by the Graph Neural Network D-GIN [19]

no antiviral activity against the CHIKV, whereas the shortened methylamine counterpart **27** was still active. Based on these findings, further analogues with shorter side chains but without H-bonding capability were investigated. Compared to their ethylamine counterparts **31b** and **34** a 10-fold loss of activity was observed within the nitrogen P3/5 dimethylamine-analogues **43a-b**, respectively. Moreover, combined with the original nitrogen positions (P1/3), the dimethylamine variation led to a loss of activity in **42b** (**Table 2**). Further, a small set of analogues without the hydrogen bond capability of the ethylamine (replaced by chloride) and a primary amine on position 3 showed no gain of activity (**44a-c** with the lowest EC_{50} value of $9.84 \pm 0.35\,\mu M$ of **44c**; **Table 4**), thus supporting our former results that the hydrogen bond donor (HBD) is not essential, but its pure absence seems to decrease

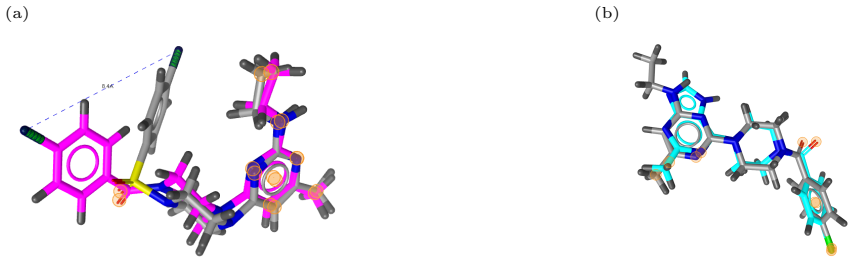

Figure 2. Minimum energy conformations after MMFF94 energy minimisation until the local minimum was reached and following alignment. (a) An example illustrating the conformational effects of amide replacement and the torsional angle difference of sulfonamide and amide scaffold.; the sulfonamide **25** (grey) shows a significant difference in structural conformation compared to the corresponding amide analogue (violet). (b) Alignment of purine-modified analogue to CHVB-compound series showing the conformational similarity of the purine-modified compound (blue) and the corresponding CHVB scaffold (grey) - resulting in similar relative positions of critical functional groups .

---

the activity.[15] Nevertheless, the possibility to replace the ethylamine with the bifurcated isopropylamine also holds true for the P3/5 nitrogen scaffold as analogue **26** gave similar antiviral results as its comparable ethylamine compound **25** (EC_{50} = 3.84 and 2.76 µM). On the other hand, the additional conversion of the sulfonamide to the amide linker in **29** resulted in an almost 6-fold decrease in activity.

Moesslacher et al. reported that the sulfonamide replacement by an amide linker enhances the activity twofold, while the methylene variation results in even more active albeit cytotoxic analogues.[15] This also holds true for most of the new designed analogues except the ones with altered or omitted pyrimidine side chains i.e. the methyl and ethylamine (e.g., **26** vs. **29**, or **15** vs. **17b**). This considerable difference in potency between the sulfonamide and its replacements (amide and methylene) may not only be the result of a possible hydrogen bond or its absence but also the consequence of a drastically different three-dimensional conformational change of the sp^3 hybridised sulfonamide and the sp^2 hybridised carboxamide. As the replacement of the linker takes place in the middle of the molecule, that torsional angle difference forces the substituted phenyl and the pyrimidine ring to change their relative distances. This may influence the desired antiviral activity since the aromatic ring with the appropriately placed substituent and the pyrimidine ring with the carefully positioned nitrogens, ethylamine chain, and methyl are most likely interacting with the target protein (nsP1) and are directly responsible for the activity (see **Figure 2a** and Molecular Docking

in Supporting Information). This hypothesis may lead further to the conclusion that the established SAR for the pyrimidine and phenyl regions of sulfonyl-analogues is *not transferable* to the amide-bearing compounds - giving an explanation why the combined optimizations with the introduction of an amide linker made by Moesslacher et al. did not give the desired gain of activity.[15]

Therefore, we shifted our focus to the phenyl substitutions in combination with the P3/5 nitrogen variation and the amide linker. To rationalise the SAR, we first evaluated **30** without any substitutions and then analyzed the effect of different electron-donating and withdrawing groups on various phenyl positions. Surprisingly, **30** was slightly more active against the CHIKV in Vero cells than our lead compound **1b** - indicating that the nitrogen shift on the pyrimidine ring has the suspected favourable impact on the activity (see **Table 2** vs. **3**). Moreover, all para-substituted analogues demonstrated a similar (**31e-f**) or even higher antiviral activity (**31a-d** and **31g**) than the un-substituted compound **30**. Especially the electron-withdrawing NO_2 and the weak deactivating halides I and Br led to a significant increase of potency with EC_{50} values of $0.91 \pm 0.18\,\mu M$, $0.70 \pm 0.28\,\mu M$, and $0.60 \pm 0.08\,\mu M$. Shifting this three promising substituents to meta position resulted only with the NO_2 modification (**32d**) in an even higher activity than the correspondent para analogues (e.g., **31d**). Nevertheless, all tested meta-substituted analogues (**32a-e**) showed strong activity.

In addition, the combined para and meta substitutions in **33a-d** achieved all similar impressive EC_{50} values around $1\,\mu M$ - with surprisingly the 3,4-dichloro substituted analogue **33a** as the most potent variation ($EC_{50} = 0.57\,\mu M$). Consequently, further di-substituted analogues with meta-meta (**34**) or ortho-para (**35a-d**) modifications were designed with two halogens, two methyl groups, and/or the Cl/NO_2 substitution. The 3,5-dichloro analogue **34** gave the most impressive antiviral activity with EC_{50} values of $0.47 \pm 0.06\,\mu M$ - an even more remarkably outcome considering that the correspondent P1/3 analogue with the same phenyl-substitutions **19** and the 2,4-dichloro analogue **35a** were completely inactive

with EC_{50} values of 66.5 and >100 µM, respectively. Further, all the ortho-para substituted compounds (**35a-d**) showed no antiviral activity. Interestingly, also the additional chloride in NO_2-substituted compounds seems not to have the desired beneficial impact on the anti-CHIKV activity as the single-substituted **32d** remains the most active of the tested NO_2 analogues (see **18b**, **32d**, **33c**, and **35b**).

Keeping these results in mind, we designed the next series of analogues with the most encouraging substitutions: i) 3,5-dichloro and 3,4-dichloro substitutions as they achieved the lowest EC_{50} values - with focus on the 3,5-dichloro variation considering the higher cytotoxicity of the 3,4-dichloro analogue **33a**, and ii) a para halide substitution as they have been demonstrating strong influence on the activity of the compound.

Purine Scaffold. The following pyrimidine modification was inspired by a major and potent class of antiviral chemotherapeutics - the nucleoside/tide analogues with the commonly used pyrimidine and purine ring system.[20,21] Moreover, the non-structural protein (nsP1) of the Chikungunya virus was determined as the main site of action of the CHVB-compound series, and almost all of the few published small molecules targeting the same viral protein contain a purine or a purine-like ring system (e.g. the MADPT-series, 6-fluoro-homoaristeromycin (FAH), 6-fluoro-homoneplanocin A (FHNA), and 5-Iodotubercidine (5-IT)).[13,16,22–24] In addition, *in silico* designed analogues in which the ethylamine side chain merges into the additional ring of the purine system showed a high structural analogy to the parent compound with all three (essential for the activity) nitrogens of the pyrimidine and ethylamine structure (see **Figure 2b**). Therefore, different analogues bearing the purine variation with various replacements for the former pyrimidine-methyl group were designed and tested. Almost none of these purine compounds showed any antiviral improvement of the anti-CHIKV activity in Vero cells. Only **45b, 46a, 46c, and 48** gave some antiviral activity - whereby **46c** gave the most interesting results with an EC_{50} value of 9.48 ± 0.39 µM and could be an interesting starting point for a new lead optimization process.

Piperazine-Bioisostere Scaffold. The final part of the SAR assessment focused on the

core region of the compound structures - the piperazine ring. Previous results with mostly sulfonamide analogues concluded that this region functions solely as a linker that keeps the needed distance between the phenyl and the pyrimidine ring - groups considered to interact most probable directly with the target protein.[15] A set of compounds with different heterocycle replacements of the piperazine ring were designed to investigate whether this conclusion still holds for analogues with an amide linker (see **Table 5**, **55a-62d**).

Analogues with an enlarged core system and a secondary amide instead of the usual tertiary amide bearing a *tert*-butyl 4-aminopiperidine-1-carboxylate (**55a-b**) or *tert*-butyl 3-aminopiperidine-1-carboxylate (**56a-b**) replacement, showed no antiviral activity. Surprisingly, moving the additional hydrogen bond donor (HBD) from the sec. amide next to the pyrimidine ring as a sec. amine, resulted in active albeit toxic and less stable **57a-b** compounds (see section *In Vitro Absorption, Distribution, Metabolism, and Excretion (ADME) Profiling*). Although the two nitrogens were retained in all three heterocycles, their relative distance increased - enlarging the area between the two main target-interacting features. To confirm whether this phenomenon was the consequence of the sec. amine and not the increased core system, analogues with the same additional HBD with the original distance between the core nitrogens as piperazine were assessed. Corresponding to the enlarged analogues, the sec. amide containing **58a-b** exhibited no antiviral activity, whereas **59b** with a sec. amine next to the pyrimidine ring was active but also unstable. From these facts, one may conclude that an additional HBD next to the pyrimidine ring is a possible variation of the lead structure, but it also leads to a decline in metabolic stability. Further, keeping a similar relative distance between the two main interacting groups as a piperazine ring also seems beneficial in combination with the amide linker. Therefore, the following compounds were designed using bridged, fused, and spiro piperazine bioisosteres with a conserved diameter and partial configuration but more rigid characteristics. From all of these compounds **61d** was the most active one with an EC_{50} value of $3.20 \pm 0.28\,\mu M$ - revealing octahydropyrrolo[3,4-c]pyrrole as a viable and interesting modification for future studies.

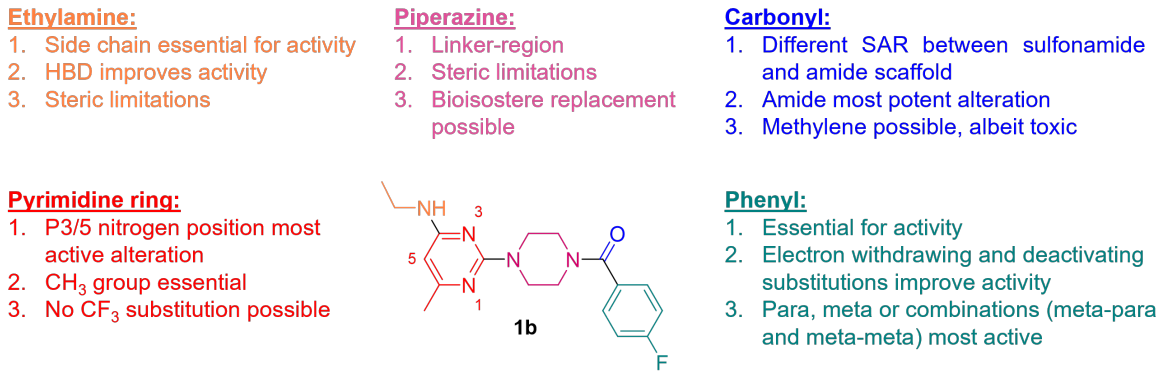

Figure 3. Summary of the structural requirements for antiviral activity described in chapter *Structure-Activity Relationship Study*.

Figure 3 summarises the structural requirements for antiviral activity described in the SAR study.

Scaffold Hopping. Taken together all the discovered requirements for a potent CHIKV-nsp1 interacting small molecule, we performed a scaffold hop for a future hit to lead drug development studies. As described above, an ethylamine sidechain- and CH_3-modifications on the pyrimidine ring are most favourable in terms of activity in combination with a P3/5 nitrogen scaffold. Considering analogues' overall much higher bioactivity with pyrimidine nitrogen P3/5 scaffold, we decided to preserve this part of the compound structure. Moreover, to keep the required relative distance and angle between the pyrimidine and the substituted phenyl regions, a quaternary carbon in the form of a spiro atom was positioned at the center of the new scaffold. This modification leads to a higher conformational rigidity and enhances the three-dimensionality of the chemical structure and hence an increased number of possible interactions with the target binding site.[25,26] Moreover, compounds with a higher fraction of sp^3 (Fsp^3) as the newly introduced spiro atom would induce, are estimated to succeed more likely in clinical trials.[27,28]

Further, by adding the carbonyl group to the chromane heterocycle, we retained the two hydrogen bond acceptors (from the carbonyl and dihydropyran) from the CHVB scaffold, which may have a positive impact on the bioactivity. The chromane was further selected for

the scaffold hop as the benzol part mirrors the former phenyl ring. The two synthesized compounds with the new scaffold **64a-b** demonstrated interesting anti-CHIKV potential (**Table 5**). According to our expectations, **64b** with the pyrimidine nitrogen pattern P3/5 was much more potent than the P1/3 variation (**64a**). With a EC_{50} value of $4.16 \pm 0.15\,\mu M$ **64b** could be a excellent starting point for a lead optimization through an additional structure-activity study.

Antiviral Profiling. The CHVB-series has been identified as a selective Chikungunya virus inhibitor with EC_{50} values against various CHIKV isolates (899 (laboratory), OPY1 (La Reunion), Venturini [Italy 2008], St Martin 20235 P2, St Martin 20236 P3, EFS-1 P3 Martinique, and Congo 95 [2011]) in the low micromolar range and no shown bioactivity against other alphaviruses.[16] Accordingly, the assessed second-generation CHVB compounds (**11a**, **12a**, **13**, and **31a**) demonstrated no activity against other alphaviruses (Semiliki Forest virus (Vietnam strain) and Sindbis virus (HRsp strain)) in virus-cell-based CPE-reduction assays on Vero cells. Additionally, screening for bioactivity against Human Enterovirus 71 and Zika virus in Vero cells gave negative results for the second-generation CHVB compounds (data not shown).

The anti-CHIKV activity was further confirmed in a virus yield assay in which treatment with selected CHVB compounds (**31b**, **31d**, **32d**, **34**, and **35d**) resulted in a pronounced dose-dependent reduction of viral RNA replication (**Figure 4c**). Compound **31b** had the most potent activity resulting in a >5 $\log_{10}$ reduction in intracellular CHIKV levels at the highest concentration tested ($60\,\mu M$). At the concentration of $2.22\,\mu M$, compounds **31b** and **32d** still reduced CHIKV replication with ~ 4.5 $\log_{10}$.

A mechanism of action study identified the CHIKV capping machinery as the target of the CHVB series. A CHVB-resistant variant ($CHVB^{res}$) carrying two mutations in the gene encoding nsP1 (responsible for the viral capping, S454G and W456R), one mutation in nsP2 (M703T), and one mutation in nsP3 (L494P) showed a high barrier to resistance to the first

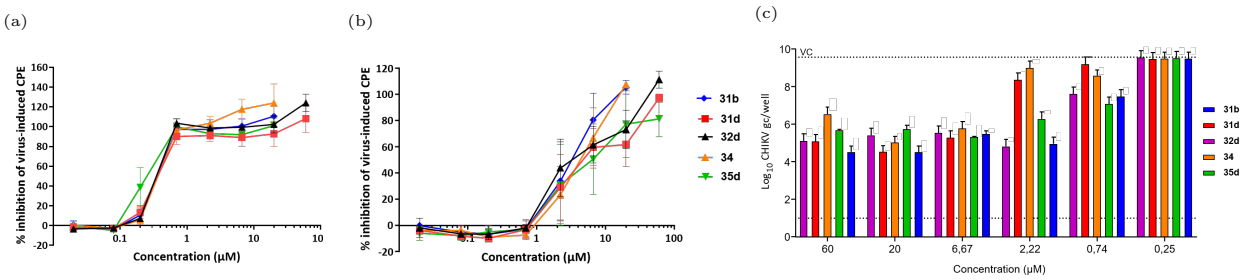

Figure 4. (a), (b): Cross-resistance of all tested CHVB compounds with the CHVB-resistant virus (CHVB^{res}). Vero cells infected with wild-type CHIKV899 (a) and CHVB^{res} (b) were assessed in a CPE reduction assay with increasing doses of selected CHVB compound. Vero cells were treated with 0 to 100 µM CHVB-compound and infected with wt or the CHIKV mutant at an MOI of 0.01. The MTS/PMS method determined the cell viability three days postinfection. Data are mean values ± SD from three independent experiments. (c): The effect of different concentrations of selected CHVB-compounds on the intracellular CHIKV RNA levels in CHIKV899-infected Vero cells (MOI, 0.01) was quantified by real-time qRT-PCR at 48 h p.i. Data shown are mean values ± SD from two independent experiments. CPE, cytopathic effect; wt, wild type; VC, virus control (untreated).

generation CHVB-compounds.[16] To investigate whether this second-generation CHVB compounds also exerted less antiviral activity against the CHVB^{res} virus, a selection of CHVB-compounds was additionally assessed for cross-resistance with CHVB^{res} (**Figure 4a** and **4b**). A similar level of resistance was measured with a fold resistance (EC_{50} CHVB^{res}/EC_{50} CHKVwt) ranging from 9.7 (**34**) up to 15 (**35d**) - suggesting that the viral capping machinery remains the main target for the optimized compounds of the CHVB series. Therefore, a molecular docking study was performed to identify possible molecular interactions and important chemical features of the CHVB compounds with their main viral target protein (nsP1, see Supporting Information).[29]

***In Vitro* Absorption, Distribution, Metabolism, and Excretion (ADME) Profiling.** The objective of discovering new analogues with improved antiviral potency over **1b** was realised for a remarkable number of compounds described above. However, high antiviral activity is one of many essential parameters in successful drug development. Therefore, to better understand the druggability of the compounds, the analogues were evaluated for their physiochemical properties and their metabolic stability in human liver microsomes (HLMs).

Physiochemical parameters, such as the aqueous solubility and $LogD_{pH\ 7.4}$, are crucial criteria in early drug design as they highly influence the absorption and distribution of the

drug.[30] Therefore, we assessed these parameters for all 100 compounds. The $LogD_{pH\ 7.4}$ value ranged from 2.40 to 3.83 (pH = 7.4). Further, the aqueous solubility at pH 7.4 differed from poor solubility (13 compounds with <50 µM) to a vast number of highly soluble compounds (56 compounds with >100 µM) including all the most potent compounds with EC_{50} values under 3 µM.

With a view to *in vivo* pharmacological experiments, we further characterised the *in vitro* microsomal half-life ($t_{1/2}$) after 60 min incubation of the compounds in human liver microsomes (HLMs). Therefore, 55 analogues were selected according to their antiviral profile and/or structural scaffold to investigate the influence of various structural changes on their pharmacokinetic profile. The results of the *in vitro* HLM metabolism study are summarised in **Table 1-5**.

The compounds showed an overall high stability with a mean half-life time of >60 min for 37 analogues. These results confirmed the previously conducted *in silico* investigation, in which all 100 compounds were screened according to their metabolic stability - revealing possible sites of metabolism (SoMs) such as the methyl and ethylamine side-chain on the pyrimidine ring.[31,32]

Scaffold-dependent metabolic stability was observed through the investigated CHVB series. All analogues with the preferable nitrogen P3/5 scaffold showed a significantly higher metabolic stability than their P1/3 counterparts (e.g., **32d** vs **18b**, and **24** vs **15**), which may indicate that the difference in local electron density (introduced by the electronegative nitrogen atoms) could influence the metabolic property. Further, almost all tested sulfonamide-analogues were not stable in human liver microsome - suggesting that the liver would rapidly metabolise them. Only in combination with the stabilising P3/5 nitrogen position in the pyrimidine ring enhanced metabolic stability could be observed within the sulfonamide analogues **24** and **27**.

A similar effect was seen within analogues without the CH_3 group at the pyrimidine ring. Both, **14** and **15** with a P1/3 scaffold were less stable than the P3/5 **23** and **24**

compounds. Interestingly, even higher stability was reached when the lacking CH_3 scaffold was combined with an amide as it is in **17a-b**. In addition, the conversion of the methyl to a trifluoromethyl showed no gain in stability (see **40a-d** and **41b**). As the introduction of a fluorine atom at the SoM is a commonly used strategy to enforce higher stability, the destabilising effect of the CF_3 group may be caused by the rupture of the C-F bond (despite its strength) during metabolism.[33–36] The two assessed purine analogues **46c** and **48** with CF_3 or Cl at the methyl position resulted, on the other hand, in a good half-life time.

Compounds with a piperazine-bioisostere scaffold showed heterogeneous results. While the primary amide compound **56b** and the sec. amine analogues **57a** and **59b** demonstrated low half-life time, all the other assessed piperazine-variations gave similar metabolic stability as the piperazine compound **34**. It is worthy to note that also the P3/5 variation of the sec. amine **57b** exhibited a $t_{1/2}$ of >60 min.

The most potent compounds (bearing a P3/5 and amide scaffold) gave a high half-life time over 60 min with the high active **31d** as the overall most stable compound (100 % compound remaining after 60 min incubation).

Toxicological Profiling. The ten most promising compounds (**31a-d**, **31g**, **32b**, **32d**, **33a**, **34**, and **35d**) were evaluated for their cytotoxic activity *in vitro* against the CaCo-2 cell line. No significant cytotoxic effects were detected (see Supporting Information). Additionaly, to analyze whether the CHVB compound series increases the expression of the apoptosis proteins caspase-3 and PARP, western blot experiments were performed with the same ten analogues. Since the caspase and PARP are apoptosis-indicating proteins, they can be used for the detection of cytotoxicity and to assess programmed cell death, respectively.[37] All compounds showed compared to the control (DMSO) neither for caspase-3 nor for PARP increased expression in all assessed concentrations. A representative blot is given in **Figure 5**.

Moreover, the Inte:Ligand Tox Pharmacophore DB was used for toxicity profiling of all

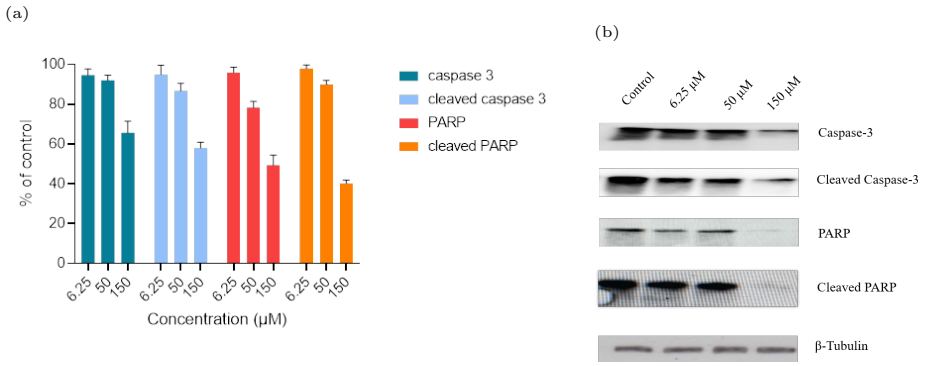

Figure 5. The assessed CHVB analogues have no increasing effect on the expression of the apoptosis proteins (cleaved caspase-3, caspase-3, cleaved PARP, and PARP). (a) Mean data of western blots of CaCo-2 cells lysate after 72 h treatment of different concentration of **32d** and control (n = 3). (b) Representative western blot from **32d**. The densitometry values were normalized to β-tubulin and set in relation to the control (DMSO).

100 synthesized compounds, but no significant effect was discovered on the hERG channel.[38] The predicted biological safety regarding possible hERG interactions was further investigated in a patch-clamp assay in Xenopus oocytes with thioridazine hydrochloride as a positive control.[39,40] A 30 % reduction of peak tail current was defined as the border for positive hERG blockade. **13** (core structure of the molecule series) was tested up to a concentration of 30 µM, showing an inhibition of 9.63 ± 5.13 % (n = 5) and thus no significant interaction above the critical defined borderlines.

Overall, neither the *in silico* nor the *in vitro* assay showed any relevant interactions of our CHVB-series with the hERG potassium channel and no significant cytotoxicity was determined - making the CHVB compound series overall a safe candidate for antiviral drug development.

Conclusion

In this study, we present the lead optimization of the CHVB-compound **1b** in light of the *in vitro* anti-CHIKV activity and ADMET profile. Further, we report an optimized synthesis route (Synthesis Route B), which improved the accessibility of the designed analogues, and the overall yield in remarkable shorter synthesis and work-up time. Altogether, 100

CHVB analogues were synthesized, tested for their antiviral activity against CHIKV by CPE-reduction assays in Vero cells, and assessed for their *in vitro* physicochemical and toxicological profile. The compounds showed overall an excellent safety profile and favourable physicochemical characteristics. The antiviral activity was confirmed in a virus yield assay. Out of this 100 novel CHVB compounds, 68 were active ($EC_{50} \leq 40\,\mu M$), 43 in a low micromolar range ($EC_{50} \leq 10\,\mu M$) and 24 more active than the initial lead compound **1b** (EC_{50} value of $3.95 \pm 0.01\,\mu M$). Moreover, 10 compounds demonstrated a remarkable high antiviral activity with EC_{50} values under $1\,\mu M$.

A thorough SAR study focusing mainly on the combination of scaffold changes revealed the structural requirement for a high antiviral activity against the CHIKV (see **Figure 3**). Of these requirements, the positions of the nitrogens in the pyrimidine ring in combination with a sulfonamide or an amide bridge significantly impacted the biological activity. Interestingly, a structure-metabolism relationship study (SMR) identified the same functional groups as the SAR study to be highly influential in metabolic stability - making the most active compounds the most stable. Hence, the discussed analogues can be categorized according to their positioning of the nitrogens in the pyrimidine ring (P1/3, P3/5, and P1/5) and whether their scaffold has a sulfonamide or an amide.

Furthermore, a cross-resistance study confirmed the viral capping machinery to be the viral target of these second-generation CHVB compounds. An additional molecular docking study showed possible interactions between the compound series and their biological target protein (nsP1, Supporting Information). Neither hERG channel interactions nor *in vitro* cytotoxicity in CaCo-2 cells was detected for this compound series - making this compound series an overall safe candidate for further *in vivo* studies.

Together, these data identify five compounds, namely **31b**, **31d**, **32d**, **34**, and **35d**, as highly potent, safe, and stable lead compounds for further development as antiviral inhibitors

of the CHIKV. Of all promising new lead compounds, **32d** demonstrates the most druggable characteristics throughout all assessed assays. Finally, the collected insight and knowledge led to a successful scaffold hop (**64b**) for future antiviral research studies.

Experimental

Chemistry Materials and General Analytical Methods. All reagents and solvents (of analytical and HPLC grades) were purchased from Sigma-Aldrich or other commercial suppliers like Fluka and Alfa Aesar and were used without further purification. Moisture-sensitive reactions were performed using anhydrous solvents and under an argon atmosphere. EtOH, THF and DCM were dried before use. Disposable needles and syringes (B— Braun Inject and B— Braun Sterican®) were applied to transfer the solvents into the reaction flask. The solvents were removed under reduced pressure using the Heildolph Laborota 4000 efficient evaporator. Analytical thin-layer chromatography (TLC) was carried out on Polygram® SIL G/UV254 plates, layer 0.2 mm silica gel with fluorescent indicator. The spots were visualised by UV light (254 and 366 nm) with CAMAG UV Lamp 4. A part of the syntheses was performed in Cem Discover to obtain microwave conditions. Compounds were purified, performing a flash chromatography on a glass column using Merck silica gel ($40-60$ mesh) or on the Biotage® Isolera™ One System. The solvent mixtures for chromatography are always referred to as a vol/vol ratio, and the melting points were determined on Cambridge Instruments.

NMR spectra were recorded on a Bruker Avance 500 NMR spectrometer (UltraShield) using a 5 mm switchable probe (TCI Prodigy Kryo-probe head, 5 mm, triple resonance-inverse-detection probe head) with z-axis gradients and automatic tuning and matching accessory (Bruker BioSpin). The resonance frequency for ^{1}H NMR was 500.13 MHz and for ^{13}C NMR 125.75 MHz. All measurements were performed for a solution in fully deuterated dimethylsulfoxide at 298 K. Standard 1D and gradient-enhanced 2D experiments, like double

quantum filtered (DQF) COSY, HSQC, and HMBC, were used as supplied by the manufacturer. Chemical shifts are referenced internally to the residual, non-deuterated solvent signal ^{1}H (δ 2.50 ppm) and the carbon signal ^{13}C (δ 39.50 ppm) of dimethylsulfoxide. ^{19}F NMR spectra were recorded on a Bruker Avance III 400 NMR spectrometer (UltraShield) using a 5 mm switchable probe (BBFOPLUS, BB/19F – 1H/D) with z-axis gradients and automatic tuning and matching accessory (Bruker BioSpin). The resonance frequency for ^{1}H NMR was 400.23 MHz and for ^{19}F NMR 376.55 MHz. All measurements were performed for a solution in fully deuterated dimethylsulfoxide at 298 K. ^{19}F NMR spectra (broadband decoupled for 1H) were measured as supplied by the manufacturer using absolute referencing via Ξ ratio. Chemical shifts are given in ppm and are reported relative to TMS and referenced to the residual proton signal of d6-DMSO (2.50 ppm). d6-DMSO with 0.03 % TMS (V/V), purchased at Euriso-top®, was used as a solvent for the samples. The specified abbreviations were used to characterize the signals: s = singlet, d = doublet, t = triplet, q = quartet, quint = quintet, sext = sextet, m = multiplet, and br = broad signal. The spectra were analysed by a computer using the software MestReNova 6 (Mestrelab research, 1994).

HRESIMS spectra were obtained on a maXis HD ESI-Qq-TOF mass spectrometer (Bruker Daltonics, Bremen, Germany). Samples were dissolved to 20 µg/mL in MeOH and directly infused into the ESI source at a flow rate of 3 µL/min with a syringe pump. The ESI ion source was operated as follows: capillary voltage: 0.9 to 4.0 kV (individually optimized), nebulizer: 0.4 bar (N_2), dry gas flow: 4 L/min (N_2), and dry temperature: 200 °C. Mass spectra were recorded in the range of m/z 50 to 1550 in the positive-ion mode. The sum formulas were determined using Bruker Compass DataAnalysis 4.2 based on the mass accuracy ($\Delta m/z \leq 2$ ppm) and isotopic pattern matching (SmartFormula algorithm).

The purity of the compounds was determined by HPLC on LC-2010A HT Liquid Chromatograph device (Shimadzu Corporation, Tokyo, Japan). The separation was carried out on an Acclaim 120 C18, 2.1 × 150 mm, 3 µm HPLC column (Thermo Fisher Scientific) using LCMS-grade water with 0.1 % FA and acetonitrile with 0.1 % FA as mobile phase A and

B, respectively. The sample components were separated and eluted with a linear gradient from 5 to 95 % B in 30 min, followed by an isocratic column cleaning and re-equilibration step. The flow rate was 0.1 mL/min, and the column oven temperature was set to 25 °C. The purity was determined from the UV chromatogram (254 nm) as the ratio of the peak area of the compound to the total peak area (i.e., the sum of the areas of all peaks that were not present in the solvent blank). Based on the HPLC data, all final compounds are ≥95 % pure.

General Synthetic Procedures.

Arylamine alkylation reaction for the synthesis of pyrimidine amines 3a-h and 9a-h can be performed according to General Synthetic Procedure A1 or General Synthetic Procedure A2.

General Synthetic Procedure A1. A stirred solution of pyrimidine (1 equiv) in anhydrous ethanol under an inert atmosphere was cooled to 0 °C before amine (2 equiv) was added dropwise. The reaction mixture was brought to room temperature and stirred for 48 hours. After evaporating the solvent, the residue was dissolved in dichloromethane and washed twice with water and brine. The organic layer was dried over sodium sulphate and then evaporated to dryness. To afford the desired pyrimidine amines, the crude product was purified by column chromatography (SiO_2, eluent: hexane/EtOAc or DCM/MeOH).

General Synthetic Procedure A2. A stirred solution of pyrimidine (1 equiv) in anhydrous THF under an inert atmosphere was cooled to 0 °C before amine (2 equiv) was added dropwise. The reaction mixture was brought to room temperature and stirred for 14 hours. After evaporation of the solvent, the residue was dissolved in dichloromethane and washed twice with H_2O and brine. The organic layer was dried over sodium sulphate and then evaporated to dryness. To afford the desired pyrimidine amines, the crude product was purified by column chromatography (SiO_2, eluent: DCM/MeOH).

Synthesis Route A

General Synthetic Procedure B: Synthesis of compounds 4a-d, 20a-20e, and 37. The pyrimidine amine **3a-h**/**9a-h** (1 equiv) and the Boc-protected pyridine **2** (2 equiv) were dissolved/suspended in 1.5 mL dry ethanol. The mixture was heated to 155 °C for 30 minutes under microwave irradiation (250 Watt, 12 bars). After the solvent was evaporated, the resulting crude product was dissolved in dichloromethane and washed twice with K_2CO_3 solution (10 % in water) and with water. The organic layer was dried over sodium sulphate, filtered, and then evaporated to dryness. To obtain the pure product, the crude was purified by column chromatography (SiO_2, eluent: 80% dichloromethane/20% methanol).

General Synthetic Procedure C: Acid-catalysed deprotection of tert-butoxycarbonyl-protected amines 5a-d, 21a-e, and 38. Carboxylate (1 equiv) was dissolved in dry tetrahydrofuran and stirred at room temperature, and then the hydrochloric acid solution (4.0 M in dioxane, 10 equiv) was added dropwise. The mixture was stirred for 24 hours and evaporated to dryness. The residuum was dissolved in dichloromethane, washed twice with an aqueous solution of potassium carbonate (10 %) and with water. The organic phase was dried over sodium sulphate and filtered to obtain the desired product.

General Synthetic Procedure D: Acylation reaction of nitrogen heterocycles. The pyrimidine (1 equiv) was dissolved in DCM. Sulfonyl chloride/benzoyl chloride (1 equiv) and triethylamine (1 equiv) as a base was added and stirred overnight at room temperature. The mixture was diluted in DCM and washed twice with H_2O and brine. The organic layer was dried over Na_2SO_4, filtered and concentrated in vacuum. The crude product was purified by recrystallization (DIPE/EtOAc; DIPE/EtOH or Hexane/EtOAc) or by column chromatography (SiO_2, eluent: DCM/MeOH).

Synthesis Route B

General Synthetic Procedure E: Nucleophilic acyl substitution for the synthesis of 6a-f and 53a-k. To a stirring solution of N-BOC-protected aminopiperazine/piperidines

(1 equiv) in pyridine, 0.006 equiv of DMAP was added. The solution was cooled down to 0 °C, and the benzoyl chloride (1.5 equiv) was added dropwise over 5 minutes. The reaction mixture was brought to room temperature and stirred for 15 hours. The crude was poured on ice, and the precipitated solid was collected by vacuum filtration and dried.

General Synthetic Procedure F: Acid-catalysed deprotection of tert-butoxycarbonyl-protected amines 7a-f and 54a-k. The boc-deprotection was performed similarly as in Synthesis Route A (General Synthetic Procedure C). After cooling down the dissolved intermediate to 0 °C TFA (50 equiv) was added. The reaction mixture was brought to room temperature and stirred for 15 hours. The solvent was evaporated, and the residue was re-dissolved in DCM. The organic layer was washed with saturated $NaHCO_3$ and H_2O, dried over sodium sulphate, and filtered to obtain the desired product.

General Synthetic Procedure G: Amination of aryl halides. The pyrimidine amine (**3a-h**/**9a-h**, 1 equiv) and the piperazine/pyridine (1-2 equiv) were dissolved/suspended with TEA (15-30 equiv) in 1.5 mL dry EtOH under inert atmosphere. The mixture was heated to 155 °C for 30 minutes under microwave irradiation (250 Watt, 12 bars). After the solvent was evaporated, the resulting crude was dissolved in dichloromethane and washed twice with K_2CO_3 solution (10 % in water) and H_2O. The organic layer was dried over sodium sulphate, filtered, and evaporated to dryness. The crude was purified by flash column chromatography (SiO_2, eluent: gradient from 0 to 15 % MeOH in DCM) to obtain the pure product.

Characterization and Spectral Data.

(4-chlorophenyl)(4-(4-(ethylamino)-6-methylpyrimidin-2-yl)piperazin-1-yl)methanone (10a). Compound **10a** was prepared following General Synthetic Procedure D using **5a** (150 mg, 0.68 mmol), 4-chlorobenzoyl chloride (118 mg, 0.67 mmol) and TEA (69 mg, 0.68 mmol) in DCM. The crude product was purified by recrystallization (DIPE/EtOAc), resulting in 123 mg of pure product (yield 50 %) as white solid.

Mp 142.4 to 144.1 °C. Ret. Time 13.41 min, purity 99.0 %. HRESIMS *m/z* 360.1588 $[M+H]^+$ (calcd for $C_{18}H_{23}ClN_5O_2^+$, 360.1586, Δ = -0.7 ppm). ^{1}H NMR (500 MHz, d_6DMSO) δ = 1.08 (t, 3H, CH_3), 2.04 (s, 3H, pyr-CH_3), 3.22 (br, 2H, NCH_2), 3.34-3.73 (br, 4H, pip-H2,6), 3.64 (br, 4H, pip-H3,5), 5.63 (s, 1H, pyr-H), 6.84 (br, 1H, NH), 7.46 (m, 2H, Ph-H2,6), 7.52 (m, 2H, Ph-H3,5). ^{13}C NMR (125 MHz, d_6DMSO) δ = 14.73 (CH_3), 23.83 (pyr-CH_3), 34.90 (NCH_2), 41.76/43.61 (pip- C3,5), 43.09/47.17 (pip-C2,6), 94.61 (pyr-C5), 128.61 (Ph-C3,5), 129.15 (Ph-C2,6), 134.29 (Ph-C4), 134.74 (Ph-C1), 161.13 (pyr-C2), 163.03 (pyr-C6), 168.21 (amide-C), n.d. (pyr-C4).

(4-bromophenyl)(4-(4-(ethylamino)-6-methylpyrimidin-2-yl)piperazin-1-yl)methanone (10b). Compound **10b** was prepared following General Synthetic Procedure D using **5a** (57 mg, 0.3 mmol), 4-bromobenzoyl chloride (84.9 mg, 0.39 mmol, 1.5 equiv) and TEA (31 mg, 0.3 mmol) in DCM. The crude product was by column chromatography (SiO_2, eluent: DCM/MeOH), resulting in 24 mg of pure product (yield 23 %) as white solid.

Mp 74 to 77 °C. Ret. time. 14.17 min, purity 95.6 %. HRESIMS *m/z* 404.1084 $[M+H]^+$ (calcd for $C_{18}H_{23}BrN_5O^+$, 404.1080, Δ = -0.8 ppm). ^{1}H NMR (500 MHz, d_6DMSO) δ = 1.08 (t, 3H, CH_3), 2.05 (s, 3H, pyr-CH_3), 3.23 (br, 2H, NCH_2), 3.65 (d, 4H, pip-H3,5), 3.73 (d, 4H, pip-H2,6), 5.63 (s, 1H, pyr-H5), 6.84 (br, 1H, NH), 7.39 (d, 2H, Ph-H2,6), 7.66 (d, 2H, Ph-H3,5). ^{13}C NMR (125 MHz, d_6DMSO) δ = 14.65 (CH_3), 23.79 (pyr-CH_3), 34.63 (NCH_2), 43.33 (pip-C2,6), 43.33 (pip-C3,5), 122.93 (Ph-C4), 129.29 (Ph-C2,6), 131.44 (Ph-C3,5), 135.07 (Ph-C1), 168.14 (amide-C), n.d. (pyr-C2), n.d. (pyr-C4), n.d. (pyr-C5), n.d. (pyr-C6).

(4-(4-(ethylamino)-6-methylpyrimidin-2-yl)piperazin-1-yl)(4-iodophenyl)methanone (10c). Compound **10c** was prepared following General Synthetic Procedure D using **5a** (200 mg, 0.9 mmol), 4-iodoobenzoyl chloride (240 mg,

0.9 mmol) and TEA (100 mg, 0.9 mmol) in DCM. The crude product was purified by column chromatography (SiO_2, eluent: DCM/MeOH) resulting in 152 mg of pure product (yield 37 %) as white/yellow solid.

MP 86 to 88 °C. Ret. time. 13.42 min, purity 96.5 %. HRESIMS m/z 452.0955 $[M+H]^+$ (calcd for $C_{18}H_{23}IN_5O^+$, 452.0942, Δ = -2.9 ppm). ^{1}H NMR (500 MHz, d_6DMSO) δ = 1.08 (t, 3H, CH_3), 2.05 (s, 3H, pyr-CH_3), 3.22 (br, 2H, NCH_2), 3.63 (d, 4H, pip-H3,5), 3.73 (d, 4H, pip-H2,6), 5.62 (s, 1H, pyr-H5), 6.84 (br, 1H, NH), 7.23 (d, 2H, Ph-H2,6), 7.83 (d, 2H, Ph-H3,5). ^{13}C NMR (125 MHz, d_6DMSO) δ = 14.68 (CH_3), 23.80 (pyr-CH_3), 34.68 (NCH_2), 43.11 (pip-C2,6), 43.49 (pip-C3,5), 96.46 (Ph-C4), 129.18 (Ph-C2,6), 135.35 (Ph-C1), 137.25 (Ph-C3,5), 161.06 (pyr-C4), 163.17 (pyr-C6), 168.36 (amide-C), n.d. (pyr-C2), n.d. (pyr-C5).

1-(4-(4-(ethylamino)-6-methylpyrimidin-2-yl)piperazin-1-yl)butan-1-one (11a). Compound **11a** was prepared following General Synthetic Procedure D using **5a** (100 mg, 0.45 mmol), butyryl chloride (49 mg, 0.45 mmol) and TEA (46 mg, 0.45 mmol) in DCM. The crude product was purified by column chromatography (SiO_2, eluent: DCM/MeOH, 8:2), resulting in 50 mg of pure product (yield 38 %) as white/yellow solid.

Mp 77 %. Ret. Time 10.66 min, purity 96.4 %. HRESIMS m/z 292.2139 $[M+H]^+$ (calcd for $C_{15}H_{26}N_5O_2^+$, 292.2132, Δ = -2.4 ppm). ^{1}H NMR (500 MHz, d_6DMSO) δ = 0.89 (t, 3H, CH_3), 1.09 (t, 3H, CH_3), 1.52 (m, 2H, CH_2), 2.05 (s, 3H, pyr-CH_3), 2.31 (t, 2H, CH2), 3.24 (br, 2H, NCH_2), 3.45-3.46 (m, 4H, pip-H2,6), 3.60-3.66 (m, 4H, pip-H3,5), 5.62 (s, 1H, pyr-H), 6.82 (br, 1H, NH). ^{13}C NMR (125 MHz, d_6DMSO) δ = 13.91 (C4), 14.74 (CH_3), 18.29 (C3), 23.84 (pyr-CH_3), 34.35 (C2), 34.79 (NCH_2), 40.98/44.91 (pip- C2,6), 43.24/43.68 (pip-C3,5), 94.08 (pyr-C5), 161.15 (pyr-C2), 163.03 (pyr-C6), 170.79 (amide-C), n.d. (pyr-C4).

cyclohexyl(4-(4-(ethylamino)-6-methylpyrimidin-2-yl)piperazin-1-yl)methanone (11b). Compound **11b** was prepared following General Synthetic Procedure D using **5a** (100 mg, 0.45 mmol), cyclohexanecarbonyl chloride (82 mg,

0.55 mmol) and TEA (46 mg, 0.45 mmol) in DCM. The crude product was purified by column chromatography (SiO_2, eluent: DCM/MeOH, 8:2), resulting in 67 mg of pure product (yield 45 %) as white/yellow solid.

Mp resinous substance. Ret. Time 14.06 min, purity 95.8 %. HRESIMS m/z 332.2406 $[M+H]^+$ (calcd for $C_{18}H_{29}N_5O^+$, 332.2411, Δ = -1.4 ppm). ^{1}H NMR (500 MHz, d_6DMSO) δ = 1.08 (t, 3H, CH_3), 1.12/1.60 (m, 2H, cyc-H4), 1.26/1.76 (m, 4H, cyc-3,5), 1.35/1.98 (m, 4H, cyc-H2,6), 2.05 (s, 3H, pyr-CH_3), 3.12 (m, 1H, cyc-H1), 3.23 (t, 2H, NCH_2), 3.24 (t, 4H, pip-H3,5), 3.69 (t, 4H, pip-H2,6), 5.63 (s, 1H, pyr-H), 6.86 (br, 1H, NH); ^{13}C NMR (125 MHz, d_6DMSO) δ = 14.71 (CH_3), 23.81 (pyr-CH_3), 24.55 (cyc-C3,5), 24.86 (cyc-C4), 26.28 (cyc-C2,6), 34.68 (NCH_2), 43.73 (pip-C2,6), 45.58 (pip- C3,5), 59.33 (cyc-C1), 94.22 (pyr-C5), 163.03 (pyr-C6), 160.98 (amide-C), n.d. (pyr-C2), n.d. (pyr-C4).

N-ethyl-6-methyl-2-(4-(propylsulfonyl)piperazin-1-yl)pyrimidin-4-amine (12a). Compound **12a** was prepared following General Synthetic Procedure D using **5a** (100 mg, 0.45 mmol), propane-1-sulfonyl chloride (64 mg, 0.45 mmol) and TEA (46 mg, 0.45 mmol) in DCM. The crude product was purified by column chromatography (SiO_2, eluent: DCM/MeOH, 8:2), resulting in 55 mg of pure product (yield 37 %) as white solid.

Mp 114 °C. Ret. time 11.90 min, purity 97.3 %. HRESIMS m/z 328.1809 $[M+H]^+$ (calcd for $C_{14}H_{26}N_5O_2S^+$, 328.1802, Δ = -2.3 ppm). ^{1}H NMR (500 MHz, d_6DMSO) δ = 0.97 (t, 3H, propyl-CH_3), 1.09 (t, 3H, CH_3), 1.69 (s, 2H, propyl-CH22), 2.05 (m, 3H, pyr-CH_3), 3.00 (m, 2H, propyl-CH2), 3.15 (m, 4H, pip-H3,5), 3.23 (br, 2H, NCH_2), 3.73 (m, 4H, pip-H2,6), 5.63 (s, 1H, pyr-H), 6.85 (br, 1H, NH). ^{13}C NMR (125 MHz, d_6DMSO) δ = 14.71 (CH_3), 12.93 (propyl-C3), 16.37 (propyl-C2), 23.82 (pyr-CH_3), 34.67 (NCH_2), 43.18 (pip-C2,6), 45.23 (pip-C3,5), 48.88 (propyl-C1), 94.29 (pyr-C5), 160.97 (pyr-C2), 163.06 (pyr-C6), n.d. (pyr-C4).

N-ethyl-6-methyl-2-(4-(naphtalen-2-ylsulfonyl)piperazin-1-yl)pyrimidin-4-amine (12b). Compound **12b** was prepared following General Synthetic Procedure D

using **5a** (100 mg, 0.45 mmol), naphtalene-2-sulfonyl chloride (105 mg, 0.46 mmol) and TEA (46 mg, 0.45 mmol) in DCM. The crude product was purified by recrystallization (DIPE/EtOAc), resulting in 60 mg of pure product (yield 32 %) as white solid.

Mp 180.7 °C. Ret. time 15.91 min, purity 97.2 %. HRESIMS m/z 412.1810 $[M+H]^+$ (calcd for $C_{21}H_{26}N_5O_2S^+$, 412.1802, Δ = -2.1 ppm). ^{1}H NMR (500 MHz, d_6DMSO) δ = 1.03 (t, 3H, CH_3), 1.97 (s, 3H, pyr-CH_3), 2.96 (m, 4H, pip-3,5), 3.16 (br, 2H, NCH_2), 3.74 (m, 4H, pip-H2,6), 5.55 (s, 1H, pyr-H), 6.80 (br, 1H, NH), 7.69 (ddd, 1H, J = 8.1 Hz, 4.9 Hz, 1.3 Hz, nap-H7), 7.73 (ddd, 1H, J = 8.1 Hz, 6.9 Hz, 1.4 Hz, nap-H6), 7.77 (dd, 1H, J = 8.7 Hz, 1.9 Hz, nap-H3), 8.07 (d, 1H, J = 8.1 Hz, nap-H5), 8.15 (d, 1H, J = 8.7 Hz, nap-H4), 8.21 (d, 1H, J = 8.1 Hz, nap-H8), 8.44 (d, 1H, J = 1.9 Hz, nap-H1). ^{13}C NMR (125 MHz, d_6DMSO) δ = 14.58 (CH_3), 23.67 (pyr-CH_3), 34.54 (NCH_2), 42.50 (pip-C2,6), 45.87 (pip-C3,5), 94.08 (pyr-C5), 122.89 (nap-C3), 127.70 (nap-C7), 127.90 (nap-C5), 128.84 (nap-C1), 129.08 (nap-C6), 129.38 (nap-C4), 129.38 (nap-C8), 132.12 (nap-C2), 131.79 (nap-C8a), 134.46 (nap-C4a), 160.61 (pyr-C2), 162.88 (pyr-C6), n.d. (pyr-C4).

N-ethyl-6-methyl-2-(4-(thiophen-2-ylsulfonyl)piperazin-1-yl)pyrimidin-4-amine (12c). Compound **12c** was prepared following General Synthetic Procedure D using **5a** (100 mg, 0.45 mmol), thiophene-2-sulfonyl chloride (83 mg, 0.46 mmol) and TEA (46 mg, 0.45 mmol) in DCM. The crude product was purified by recrystallization (DIPE/EtOAc), resulting in 25 mg of pure product (yield 15 %) as white/yellow solid.

Mp 160.4 to 171.1 °C. Ret. time 13.55 min, purity 96.1 %. HRESIMS m/z 368.1218 $[M+H]^+$ (calcd for $C_{15}H_{22}N_5O_2S^+$, 368.1209, Δ = -2.4 ppm). ^{1}H NMR (500 MHz, d_6DMSO) δ = 1.06 (t, 3H, CH_3), 2.02 (s, 3H, pyr-CH_3), 2.92 (m, 4H, pip-H3,5), 3.20 (br, 2H, NCH_2), 3.77 (m, 4H, pip-H2,6), 5.60 (s, 1H, pyr-H), 6.86 (br, 1H, NH), 7.28 (dd, 1H, J = 8.8 Hz, th-H4), 7.65 (dd, 1H, J = 5.1 Hz, th-H3), 8.05 (dd, 1H, J = 6.3 Hz, th-H5). ^{13}C NMR (125 MHz, d_6DMSO) δ = 14.61 (CH_3), 23.69 (pyr-CH_3), 34.56 (NCH_2), 42.38 (pip-C2,6), 45.79 (pip-C3,5), 94.55 (pyr-C5), 128.42 (th-C4), 133.25 (th-C3), 134.03 (th-C5), 134.45 (th-C2), 160.71 (pyr-C2), 162.94 (pyr-C6), 174.77 (pyr-C4).

2-(4-((6-chloropyridin-3-yl)sulfonyl)piperazin-1-yl)-N-ethyl-6-methylpyrimidin-4-amine (12d). Compound **12d** was prepared following General Synthetic Procedure D using **5a** (100 mg, 0.45 mmol), 6-chloropyridine-3-sulfonyl chloride (109 mg, 0.52 mmol) and TEA (46 mg, 0.45 mmol) in DCM. The crude product was purified by recrystallization (DIPE/EtOAc), resulting in 106 mg of pure product (yield 59 %) as white/yellow solid.

Mp 179.8 to 180.6 °C; Ret. time 13.61 min, purity 95.9 %. HRESIMS m/z 397.1220 $[M+H]^+$ (calcd for $C_{16}H_{22}ClN_6O_2S^+$, 397.1208, Δ = -3.1 ppm). ^{1}H NMR (500 MHz, d_6DMSO) δ = 1.06 (t, 3H, CH_3), 2.01 (s, 3H, pyr-CH_3), 2.99 (m, 4H, pip-H3,5), 3.19 (br, 2H, NCH_2), 3.76 (m, 4H, pip-H2,6), 5.59 (s, 1H, pyr-H), 6.84 (br, 1H, NH), 7.78 (dd, 1H, J = 8.8 Hz, pyridine-H5), 8.18 (dd, 1H, J = 11.0 Hz, pyridine-H4), 8.75 (dd, 1H, J = 3.0 Hz, pyridine-H2). ^{13}C NMR (125 MHz, d_6DMSO) δ = 14.62 (CH_3), 23.70 (pyr-CH_3), 34.48 (NCH_2), 42.39 (pip-C2,6), 45.58 (pip-C3,5), 94.41 (pyr-C5), 125.40 (pyridine-C5), 131.26 (pyridine-C3), 138.95 (pyridine-C4), 148.55 (pyridine-C2), 154.57 (pyridine-C6), 160.59 (pyr-C2), 162.94 (pyr-C6), 174.29 (pyr-C4).

2-(4-((4-fluorophenyl)sulfonyl)piperazin-1-yl)pyrimidine (13). Compound **13** was prepared following General Synthetic Procedure D using 2-(piperazin-1-yl)pyrimidine (127 mg, 0.77 mmol), 4-fluorobenzenesulfonyl chloride (150 mg, 0.77 mmol) and TEA (78 mg, 0.78 mmol) in DCM. The crude product was purified by column chromatography (SiO_2, eluent: DCM/MeOH, 9:1), resulting in 215 mg of pure product (yield 86 %) as white solid.

Mp 198.4 to 200.0 °C. Ret. Time 23.46 min, purity 98.0 %. HRESIMS m/z 323.0972 $[M+H]^+$ (calcd for $C_{14}H_{16}FN_4O_2S^+$, 323.0973, Δ = -0.1 ppm). ^{1}H NMR (500 MHz, d_6DMSO) δ = 2.95 (t, 4H, pip-H3,5), 3.82 (t, 4H, pip-H2,6), 6.64 (t, 1H, pyr-H5), 7.47 (m, 2H, Ph-3,5), 7.82 (m, 2H, Ph-H2,6), 8.33 (d, 2H, pyr-H4,6). ^{13}C NMR (125 MHz, d_6DMSO) δ = 42.58 (pip-C2,6), 45.68 (pip- C3,5), 110.81 (pyr-C5), 116.79 ($^3J(^{13}C,^{19}F)$ = 22.3 Hz, Ph-C3,5),

130.75 (^{3}J(^{13}C,^{19}F) = 9.4 Hz, Ph-C2,6), 131.20 (^{3}J(^{13}C,^{19}F) = 3.1 Hz, Ph-C1), 158.09 (pyr-C4,6), 160.84 (pyr-C2), 164.79 (^{3}J(^{13}C,^{19}F) = 250.49 Hz, Ph-C4). ^{19}F NMR (376.55 MHz, d_6DMSO) δ = -105.56 (Ph-F).

2-(4-((4-fluorophenyl)sulfonyl)piperazin-1-yl)-N-isopropylpyrimidin-4-amine (14). Compound **14** was prepared following General Synthetic Procedure D using **5b** (86 mg, 0.39 mmol), 4-fluorobenzenesulfonyl chloride (75 mg, 0.38 mmol) and TEA (40 mg, 0.39 mmol) in DCM. The crude product was purified by column chromatography (SiO_2, eluent: DCM/MeOH, 8:2), resulting in 98 mg of pure product (yield 67 %) as white solid.

Mp 147 °C. Ret. Time 13.25 min, purity 98.5 %. HRESIMS m/z 380.1558 $[M+H]^+$ (calcd for $C_{17}H_{23}FN_5O_2S^+$, 380.1551, Δ = -1.9 ppm. ^{1}H NMR (500 MHz, d_6DMSO) δ = 1.09 (d, 3H, ipr-CH_3), 2.91 (t, 4H, pip-H3,5), 3.74 (t, 4H, pip-H2,6), 4.00 (br, 1H, ipr-H), 5.75 (d, 1H, pyr-H5), 7.13 (br, 1H, NH), 7.47 (t, 2H, Ph-3,5), 7.63 (s, 1H, pyr-H6), 7.82 (q, 2H, Ph-H2,6). ^{13}C NMR (125 MHz, d_6DMSO) δ = 22.30 (ipr-CH_3), 41.37 (ipr-CH), 42.64 (pip-C2,6), 45.68 (pip- C3,5), 96.74 (pyr-C5), 116.77 (^{3}J(^{13}C,^{19}F) = 22.7 Hz, Ph-C3,5), 130.77 (^{3}J(^{13}C,^{19}F) = 9.7 Hz, Ph-C2,6), 131.15 (^{3}J(^{13}C,^{19}F) = 2.4 Hz, Ph-C1), 161.58 (pyr-C4), 164.78 (^{3}J(^{13}C,^{19}F) = 250.6 Hz, Ph-C4), n.d. (pyr-C2), n.d. (pyr-C6). ^{19}F NMR (376.55 MHz, d_6DMSO) δ = -105.55 (Ph-F).

2-(4-((4-chlorophenyl)sulfonyl)piperazin-1-yl)-N-ethylpyrimidin-4-amine (15). Compound **15** was prepared following General Synthetic Procedure D using **5c** (88 mg, 0.42 mmol), 4-chlorobenzenesulfonyl chloride (90 mg, 0.42 mmol) and TEA (43 mg, 0.42 mmol) in DCM. The crude product was purified by column chromatography (SiO_2, eluent: DCM/MeOH, 8:2), resulting in 75 mg of pure product (yield 46 %) as white solid.

Mp 66.6 °C. Ret. Time 14.57 min, purity 95.8 %. HRESIMS m/z 382.1110 $[M+H]^+$ (calcd for $C_{16}H_{21}ClN_5O_2S^+$, 382.1099, Δ = -2.9 ppm). ^{1}H NMR (500 MHz, d_6DMSO) δ = 1.06 (t, 3H, CH_3), 2.90 (m, 4H, pip-H3,5), 3.20 (m, 2H, NCH_2), 3.74 (m, 4H, pip-H2,6), 5.72 (d, 1H, pyr-H5), 7.02 (br, 1H, NH), 7.64 (br, 1H, pyr-H6), 7.70 (m, 2H, Ph-H2,6), 7.75

(m, 2H, Ph-3,5). ^{13}C NMR (125 MHz, d_6DMSO) δ = 14.54 (CH_3), 34.45 (NCH_2), 42.52 (pip-C2,6), 45.76 (pip- C3,5), 96.46 (pyr-C5), 129.57 (Ph-C3,5), 129.70 (Ph-C2,6), 133.71 (Ph-C4), 138.40 (Ph-C1), 154.44 (pyr-C6), 160.77 (pyr-C2), 162.32 (pyr-C4).

2-(4-((4-fluorophenyl)sulfonyl)piperazin-1-yl)-N,6-dimethylpyrimidin-4-amine (16). Compound **16** was prepared following General Synthetic Procedure D using **5d** (83 mg, 0.4 mmol), 4-fluorobenzenesulfonyl chloride (78 mg, 0.4 mmol) and TEA (46 mg, 0.45 mmol) in DCM. The crude product was purified by recrystallization (DIPE/EtOAc), resulting in 15 mg of pure product (yield 10 %) as white solid.

Mp 126.9 to 128.4 °C. Ret. time 13.24 min, purity 95.7 %. HRESIMS m/z 366.1405 $[M+H]^+$ (calcd for $C_{16}H_{21}FN_5O_2S^+$, 3666.1395, Δ = -3.0 ppm). ^{1}H NMR (500 MHz, d_6DMSO) δ = 2.01 (s, 3H, pyr-CH_3), 2.69 (d, 3H, NCH_2), 2.88 (t, 4H, pip-H3,5), 3.75 (t, 4H, pip-H2,6), 5.59 (s, 1H, pyr-H5), 6.80 (br, 1H, NH), 7.47 (t, 2H, Ph-H3,5), 7.81 (q, 2H, Ph-H2,6). ^{13}C NMR (125 MHz, d_6DMSO) δ = 23.74 (pyr-CH_3), 26.79 (NCH_2), 42.50 (pip-C2,6), 45.87 (pip-C3,5), 94.48 (pyr-C5), 116.75 (d, $^3J(^{13}C,^{19}F)$ = 22.3 Hz, Ph-C3,5), 130.76 (d, $^3J(^{13}C,^{19}F)$ = 9.8 Hz, PH-C2,6), 131.13 (d, $^3J(^{13}C,^{19}F)$ = 2.5 Hz, Ph-C1), 160.64 (pyr-C2), 163.70 (pyr-C4), 163.77 (pyr-C6), 164.77 (d, $^3J(^{13}C,^{19}F)$ = 250.5 Hz, Ph-C4). ^{19}F NMR (376.55 MHz, d_6DMSO) δ = -105.56 (Ph-F).

(4-(4-(ethylamino)pyrimidin-2-yl)piperazin-1-yl)(4-fluorophenyl)methanone (17a). Compound **17a** was prepared following General Synthetic Procedure D using **5c** (97 mg, 0.47 mmol), 4-fluorobenzoyl chloride (74 mg, 0.47 mmol) and TEA (46 mg, 0.45 mmol) in DCM. The crude product was purified by recrystallization (DIPE/EtOAc), resulting in 50 mg of pure product (yield 32 %) as white solid.

Mp 164.8 °C. Ret. Time 14.44 min, purity 95.8 %. HRESIMS m/z 330.1733 $[M+H]^+$ (calcd for $C_{17}H_{21}FN_5O^+$, 330.1725, Δ = -2.7 ppm). ^{1}H NMR (500 MHz, d_6DMSO) δ = 1.09 (t, 3H, CH_3), 3.24 (br, 2H, NCH_2), 3.68 (br, 4H, pip-H3,5), 3.68 (br, 4H, pip-H2,6), 5.76 (d, 1H, pyr-H5), 7.02 (br, 1H, NH), 7.29 (m, 2H, Ph-3,5), 7.50 (m, 2H, Ph-H2,6), 7.70 (br, 1H, pyr-H6). ^{13}C NMR (125 MHz, d_6DMSO) δ = 14.54 (CH_3), 34.39 (NCH_2), 43.30 (pip-

C2,6), 43.30 (pip- C3,5), 96.19 (pyr-C5), 115.41 (^{3}J(^{13}C,^{19}F) = 21.3 Hz, Ph-C3,5), 129.65 (^{3}J(^{13}C,^{19}F) = 8.2 Hz, Ph-C2,6), 132.33 (^{3}J(^{13}C,^{19}F) = 3.3 Hz, Ph-C1), 154.47 (pyr-C6), 161.12 (pyr-C2), 162.29 (pyr-C4), 162.55 (^{3}J(^{13}C,^{19}F) = 245.0 Hz, Ph-C4), 168.28 (amide-C). ^{19}F (376.55 MHz, d_6DMSO) δ = -111.18 (Ph-F).

(4-chlorophenyl)(4-(4-(ethylamino)pyrimidin-2-yl)piperazin-1-yl)methanone (17b). Compound **17b** was prepared following General Synthetic Procedure D using **5c** (62 mg, 0.3 mmol), 4-chlorobenzoyl chloride (52 mg, 0.3 mmol) and TEA (31 mg, 0.3 mmol) in DCM. The crude product was purified by column chromatography (SiO_2, eluent: DCM/MeOH, 8:2), resulting in 90 mg of pure product (yield 87 %) as white solid.

Mp 185 °C. Ret. Time 13.29 min, purity 96.0 %. HRESIMS m/z 346.1436 $[M+H]^+$ (calcd for $C_{17}H_{21}ClN_5O^+$, 346.1429, Δ = -2.1 ppm). ^{1}H NMR (500 MHz, d_6DMSO) δ = 1.09 (t, 3H, NCH_3), 3.24 (br, 2H, NCH_2), 3.34/3.74 (m, 4H, pip-H2,6), 3.64 (br, 4H, pip-H3,5), 5.76 (d, 1H, pyr-H5), 7.03 (br, 1H, NH), 7.46 (m, 2H, Ph-2,6), 7.52 (m, 2H, Ph-H3,5), 7.70 (br, 1H, pyr-H6). ^{13}C NMR (125 MHz, d_6DMSO) δ = 14.60 (NCH_3), 34.49 (NCH_2), 41.70/43.59 (pip- C3,5), 43.04/47.11 (pip-C2,6), 96.32 (pyr-C5), 128.62 (Ph-C3,5), 129.14 (Ph-C2,6), 134.30 (Ph-C4), 134.74 (Ph-C1), 154.42 (pyr-C6), 161.12 (pyr-C2), 162.37 (pyr-C4), 168.24 (amide-C).

(3-bromophenyl)(4-(4-(ethylamino)-6-methylpyrimidin-2-yl)piperazin-1-yl)methanone (18a). Compound **18a** was prepared following General Synthetic Procedure D using **5a** (60 mg, 0.27 mmol), 3-bromobenzoyl chloride (87 mg, 0.4 mmol, 1.5 equiv) and TEA (27 mg, 0.27 mmol) in DCM. The crude product was purified by column chromatography (SiO_2, eluent: DCM/MeOH, 8:2), resulting in 36 mg of pure product (yield 33 %) as white solid.

Mp 152 to 153 °C. Ret. time. 14.17 min, purity 97.6 %. HRESIMS m/z 404.1092 $[M+H]^+$ (calcd for $C_{18}H_{23}BrN_5O^+$, 404.1080, Δ = -2.7 ppm). ^{1}H NMR (500 MHz, d_6DMSO) δ = 1.08 (t, 3H, CH_3), 2.05 (s, 3H, pyr-CH_3), 3.23 (br, 2H, NCH_2), 3.33-3.63 (d, 4H, pip-H2,6), 3.65-3.75 (br, 4H, pip-H3,5), 5.63 (s, 1H, pyr-H5), 6.84 (br, 1H, NH), 7.42 (d, 1H, Ph-H5), 7.43

(m, 1H, Ph-H6), 7.62 (t, 1H, Ph-H2), 7.67 (m, 1H, Ph-H4). ^{13}C NMR (125 MHz, d_6DMSO) δ = 14.67 (CH_3), 23.77 (pyr-CH_3), 34.50 (NCH_2), 41.61-43.49 (pip-C3,5), 42.97-47.04 (pip-C2,6), 121.73 (Ph-C3), 125.94 (Ph-C6), 129.64 (Ph-C2), 130.70 (Ph-C5), 132.36 (Ph-C4), 138.29 (Ph-C1), 161.06 (pyr-C2), 162.96 (pyr-C6), 167.42 (amide-C), n.d. (pyr-C4), n.d. (pyr-C5).

(4-(4-(ethylamino)-6-methylpyrimidin-2-yl)piperazin-1-yl)(3-nitrophenyl)methanone (18b). Compound **18b** was prepared following General Synthetic Procedure D using **5a** (60 mg, 0.27 mmol), 3-nitrobenzoyl chloride (49 mg, 0.27 mmol) and TEA (27 mg, 0.27 mmol) in DCM. The crude product was purified by column chromatography (SiO_2, eluent: DCM/MeOH, 8:2), resulting in 60 mg of pure product (yield 61 %) as white solid.

Mp 127 to 129 °C. Ret. time. 12.75 min, purity 95.1 %. HRESIMS m/z 371.1831 $[M+H]^+$ (calcd for $C_{18}H_{23}N_6O_3^+$, 371.1826, Δ = -1.4 ppm). ^{1}H NMR (500 MHz, d_6DMSO) δ = 1.08 (t, 3H, CH_3), 2.05 (s, 3H, pyr-CH_3), 3.23 (br, 2H, NCH_2), 3.35-3.67 (d, 4H, pip-H2,6), 3.67-3.78 (d, 4H, pip-H3,5), 5.63 (s, 1H, pyr-H5), 6.85 (br, 1H, NH), 7.76 (dd, J = 15.8 Hz, 1H, Ph-H5), 7.89 (ddd, J = 10.1 Hz, 1H, Ph-H6), 8.24 (dd, J = 3.6 Hz, 1H, Ph-H2). ^{13}C NMR (125 MHz, d_6DMSO) δ = 14.66 (CH_3), 23.76 (pyr-CH_3), 34.59 (NCH_2), 41.71-47.04 (pip-C2,6), 42.98-43.50 (pip-C3,5), 122.00 (Ph-C2), 124.28 (Ph-C4), 130.27 (Ph-C5), 133.47 (Ph-C6), 137.45 (Ph-C1), 147.70 (Ph-C3), 162.96 (pyr-C6), 166.90 (amide-C), n.d. (pyr-C2), n.d. (pyr-C4), n.d. (pyr-C5).

(3,5-dichlorophenyl)(4-(4-(ethylamino)-6-methylpyrimidin-2-yl)piperazin-1-yl)methanone (19). Compound **19** was prepared following General Synthetic Procedure D using **5a** (50 mg, 0.2 mmol), 3,5-dichlorobenzoyl chloride (63 mg, 0.34 mmol, 1.5 equiv) and TEA (27 mg, 0.27 mmol) in DCM. The crude product was purified by column chromatography (SiO_2, eluent: DCM/MeOH, 8:2), resulting in 51 mg of pure product (yield 65 %) as brown solid.

Mp 197 °C. Ret. time. 24.70 min, purity 95.2 %. HRESIMS m/z 394.1201 $[M+H]^+$ (calcd

for $C_{18}H_{22}Cl_2N_5O^+$, 394.1196, Δ = -1.4 ppm). ^{1}H NMR (500 MHz, d_6DMSO) δ = 1.08 (t, 3H, CH_3), 2.06 (s, 3H, pyr-CH_3), 3.24 (br, 2H, NCH_2), 3.32-3.63 (d, 4H, pip-H2,6), 3.66-3.75 (d, 4H, pip-H3,5), 5.64 (s, 1H, pyr-H5), 6.86 (br, 1H, NH), 7.51 (d, 2H, Ph-H2,6), 7.73 (t, 1H, Ph-H4). ^{13}C NMR (125 MHz, d_6DMSO) δ = 14.65 (CH_3), 23.73 (pyr-CH_3), 34.59 (NCH_2), 41.62-46.91 (pip-C2,6), 42.93-43.42 (pip-C3,5), 125.65 (Ph-C2,6), 129.06 (Ph-C4), 134.32 (Ph-C3,5), 139.49 (Ph-C1), 166.10 (amide-C), n.d. (pyr-C2), n.d. (pyr-C4), n.d. (pyr-C5), n.d. (pyr-6).

The characterization and spectral data of final compounds and intermediates 20a-64b are reported in Supporting Information.

Cell Lines and Virus Strains. Chikungunya virus, Indian Ocean strain 899, isolated in 2006 (Genbank FJ959103.1), was kindly provided by Prof. C. Drosten (Institute of Virology, University of Bonn, Germany). CHVB-resistant CHIKV was generated previously by passaging.[16] CHIKV was cultured on African green monkey kidney (Vero) cells (ATCC CCL-81) in minimum essential medium MEM Rega3 (Invitrogen, Belgium) supplemented with 10 % Foetal Bovine Serum (FBS; Integro, The Netherlands), 1 % L-glutamine and 1 % sodium bicarbonate (Invitrogen). Antiviral assays were performed in MEM Rega-3 medium supplemented with 2 % FBS.

Chikungunya virus-cell-based Antiviral Assay. Serial dilutions of compound were prepared in assay medium [MEM Rega3 (Cat. N°19993013; Invitrogen), 2 % FCS (Integro), 5 mL 200 mM L-glutamine (25030024), and 5 mL 7.5 % sodium bicarbonate (25080060)] that was added to empty wells of a 96-well microtiter plate (Falcon, BD). Subsequently, 50 µL of CHIKV (wt or CHVB-resistant) in assay medium was added (resulting in a MOI of 0.01), followed by 50 µL of Vero cell suspension (25 000 cells/50 µL). The assay plates were returned to the incubator (37 °C, 5 % CO_2, 95 to 99 % relative humidity) for 5 days (for the high-throughput screening) or 3 days (for the cross-resistance study), a time at which maximal virus-induced cell death or cytopathic effect (CPE) was observed in untreated, infected

controls. Subsequently, the assay medium was aspirated, replaced with 75 µL of a 5 % MTS (Promega) solution in phenol red-free medium and incubated for 1.5 hours. Absorbance was measured at a wavelength of 498 nm (Safire2, Tecan; optical densities (OD values) reached 0.6-0.8 for the untreated, uninfected controls). The EC_{50} (50 % effective concentration or concentration which is calculated to inhibit virus-induced cell death by 50 %) and CC_{50} (50 % antimetabolic concentration or concentration which is calculated to inhibit the overall cell metabolism by 50 %) values were derived from the dose-response curves. The 50 % effective concentration (EC_{50}) and the 90 % effective concentration (EC_{90}) are the concentrations of compound that inhibit virus replication by 50 % and 90 %, respectively. The overall antimetabolic effect of the compounds is shown as Cytostatic/Cytotoxic Concentration (CC_{50}). The CC_{50} is the calculated concentration of compound that causes a 50 % adverse effect on non-infected host cells (incorporates cytotoxic, cytostatic, and antimetabolic effect). All assay conditions producing an antiviral effect exceeding 50 % were checked microscopically for minor signs of CPE or adverse effects on the host cell (i.e. altered cell morphology). A compound was only considered to elicit a selective antiviral effect on virus replication when, following microscopic quality control, at least at one concentration of the compound, no CPE nor any adverse effect is observed (image resembling untreated, uninfected cells). Multiple independent experiments were performed.

Virus Yield Assay. Vero cells were seeded in 96-well plates at a density of 5×10^4 cells/well. The next day, cells were treated with serial dilutions of the compound and then infected with CHIKV-899 (MOI of 0.01). Two hours postinfection, the cells were washed to remove the nonadsorbed virus, followed by incubation with the same serial dilutions of compounds. After 48 h of incubation, viral RNA was quantified by real-time quantitative RT-PCR (qRT-PCR) as described previously.[16]

Aqueous Solubility. Samples were diluted in DMSO (control), phosphate buffer pH = 7.4 and pH = 2.0, from 5 mM stock solutions (dissolved in DMSO), to 120 µM final concentration. The samples were incubated for 24 hours at room temperature, followed by 30 minutes of centrifugation at 3700 rpm. Two individual sample solutions were made and measured.

40 µL of the supernatants were injected into HPLC (gradient elution, eluent A 0.1 % formic acid in water, eluent B acetonitrile, waters 2795 separation module and 996 PDA detector controlled by MassLynx 4.1 Column: X-Bridge C18 3.5 µm 4.6 × 50 mm) and the AUC (Absorbance Unit under the Curve) values (measured on sample-specific wavelength) of the buffered samples were divided by the AUC values (same wavelength as buffered samples) of the DMSO control samples.

***In Silico* cLogD.** The Graph Neural Network (GNN) was used for clogD calculation.[19]

***In Silico* Metabolic Stability.** The machine learning program FAst MEtabolizer 3 (FAME 3) was used for metabolic stability profiling and to assess critical sites of metabolism (SoMS).[31,32]

Metabolic Stability in Human Liver Microsomes. The stability of a test compound was determined in human liver microsomes (mixed gender and pool of 50) in 96-well plate format. The test compound is quantified at five time points by HPLC-MS/MS analysis with final microsomal protein concentration: 0.1 mg/mL and test concentration 0.1 µM with 0.01 % DMSO, 0.25 % acetonitrile and 0.25 % methanol.

The test compound is pre-incubated with pooled liver microsomes in phosphate buffer (pH 7.4) for 5 min in a 37 °C shaking water bath. The reaction is initiated by adding an NADPH-generating system and incubated for 0, 15, 30, 45 and 60 min. The reaction is stopped by transferring the incubation mixture to acetonitrile/methanol. Samples are then

mixed and centrifuged. Supernatants are used for HPLC-MS/MS analysis. Four reference compounds were used: propranolol and imipramine as relatively stable, whereas verapamil and terfenadine as readily metabolized reference compounds.

Samples are analyzed by HPLC-MS/MS using selected reaction monitoring. The HPLC system consists of a binary LC pump with an autosampler, a C-18 column, and a gradient. Peak areas corresponding to the test compound are recorded for data analysis. The compound remaining is calculated by comparing the peak area at each time point to time zero. The half-life is calculated from the slope of the initial linear range of the logarithmic curve of the compound remaining (%) vs time, assuming first-order kinetics. In addition, the intrinsic clearance (Clint) is calculated from the half-life using the following equation.

$$CLint_{(\mu L/min/mg\ protein)} = \frac{0.693}{T_{1/2} \times Protein\ Conc.}$$

***In Silico* hERG Channel Activity Profiling.** The Inte:Ligand Tox Pharmacophore DB was used for toxicity profiling of compounds within a KNIME workflow.[38,41]

***In Vitro* hERG Channel Activity Profiling.** Initial hERG Block Screening in Oocytes. Preparation of stage V–VI oocytes from Xenopus laevis (NASCO, Fort Atkinson, WI, USA), synthesis of capped runoff complementary ribonucleic acid (cRNA) transcripts from linearised complementary deoxyribonucleic acid (cDNA) templates, and injection of cRNA were performed as described previously.[40,42]

Currents through hERG channels were studied 1-3 days after cRNA injection using a two microelectrode voltage-clamp technique with a Turbo TEC-03X amplifier (npi electronic GmbH, Tamm, Germany). The extracellular recording solution contained: 96 mM NaCl, 2 mM KCl, 1 mM $MgCl_2$, 5 mM HEPES and 1.8 mM $CaCl_2$ (pH 7.5). Voltage-recording and current-injecting microelectrodes were filled with 3 M KCl and had resistances between 0.5 to 2 MΩ. Endogenous currents did not exceed 0.2 µA. Currents >3 µA were discarded to minimize voltage clamp errors. A precondition for all measurements was the achievement of

stable peak current amplitudes over periods of 10 min after an initial run-up period. Stocks were diluted in extracellular solution on the day of each experiment, and the maximal DMSO concentration (1 %) did not affect hERG currents. All compounds (30 µM) were applied by means of a fast perfusion system (ScreeningTool, npi electronic GmbH, Tamm, Germany).[39] Thioridazine hydrochloride (Sigma-Aldrich GmbH, Vienna, Austria) was used as positive control. The pClamp software package version 10.1 (Molecular Devices, Sunnyvale, CA, USA) was used for data acquisition.

Cytotoxicity Assay. Human colorectal adenocarcinoma cells CaCo-2 cells were seeded in 96 well plates at density 2000 cells/well in 100 µL/well medium and incubated for 24 hours. After that, cells were incubated with 100 µL of CHVB compound at different concentrations. The proportion of viable cells was determined after 24, 48 and 72 hours after exposure to CHVB compound by 3-(4,5-dimethylthiazol-2-yl)-2,-5 diphenyltetrazolium bromide (MTT)-based viability assay (EZ4U, Biomedica, Vienna, Austria). Briefly, 20 µL of EZ4U solution was added to each well. After incubation for 2 hours at 37 °C the absorbance was measured by a microplate reader at 450 nm with 620 nm as reference to reduce the unspecific background values. All experiments were carried out three times in triplicates.

Western Blot. Experiments were done as previously described.[43–46] Briefly, cells were grown in 100 µL cell culture dishes in 5% CO_2 incubator in DMEM medium supplemented with 5% fetal bovine serum. Medium was then aspirated, cells washed twice with PBS. Cells scrapped in lysis buffer (200 mM sodium acetate, 150 mM NaCL, pH 5.5 supplemented with 40 µM E-64 and transferred to 1.5 mL centrifuge tube. The cells were then homogenized on ice by ultrasonication then 0.1%triton X-100 were added. The homogenized cells were then extracted on ice for 30 minutes. Samples were then cleared by centrifugation 15000 x g for 10 minutes. The proteins were separated under reducing conditions by SDS-PAGE using 12.5% polyacrylamide gel along with prestained marker (cell signalling). Proteins were then transferred to nitrocellulose membrane (Santa Cruz Biotechnology) by semi-dry blot-

ting at 25 V for 30 minutes. Unspecific sites were then blocked for 3 hours by blocking solution (3% BSA in PBS). Membrane were then incubated for 90 minutes with the primary antibodies, caspase-3, cleaved caspase-3, PARP, and cleaved PARP (Thermo Fisher Scientific Inc.), washed five times with PBST and incubated another 90 minutes with the corresponding secondary antibodies and washed three times with PBST and once PBS. Enhanced chemiluminescence (Amersham ECL plus western blotting detection reagent, GE Healthcare, Vienna, Austria) was used for visualization. Membranes were exposed to X-ray films (Ammersham Hyper film ECL, GE Healthcare). Exposed films were scanned and quantified using ImageJ (NIH, Maryland, USA).

Authors Contributions

V.B. wrote the manuscript, coordinated the project, collected physiochemical, metabolic stability, and *in silico* data, and analysed the data from all reported assays; V.B. and J.M designed research project, designed synthesis routes and synthesized compounds; V.B. and E.U. analyzed identity of compounds; R.A., P.L., A.L.R.R., L.L., J.N, and L.D. performed antiviral assays; M.A, C.S, J.K, and J.R performed toxicological assays; L.D., E.U. and T.L. contributed with feedback and corrections. T.L., E.U., and G.P. supervised the project. All authors have given approval to the final version of the manuscript.

Funding Sources

This work was funded in parts (University of Innsbruck, KU Leuven, and University of Vienna) by European Union Seventh Framework Program (FP7/2007–2013) under SILVER grant (No. HEALTH-F3-2010-260644).

Notes

The authors declare no competing financial interest.

Abbreviations

CHIKV, Chikungunya virus; CHIKF, Chikungunya Fever, ADMET, absorption, distribution, metabolism, excretion, toxicity; HLM, human liver microsome; SAR, structure-activity relationship; SMR, structure-metabolism relationship; nsP1, non-structural protein 1, DMAP, 4-dimethylaminopyridine; Boc, tert-butyloxycarbonyl; TFA, trifluoroacetic acid; HCl, hydrochloric acid; DIPEA, N,N-diisopropylethylamine; THF, tetrahydrofuran; FA, formic acid; TOFA, triethyl orthoformate; DCM, dichloromethane; EtOAc, ethyl acetate; CPE, cytopathic effect; CHVBres, CHVB-resistant virus; wt, wild type.

Acknowledgement

We thank Caroline Collard for her excellent technical assistance in the acquisition of the antiviral data. Furthermore, we a grateful to J. Wackerlig and D. Dobusch for the assistance with the chemical analysis of the compounds. We further thank M. Sanguinetti (University of Utah, UT, USA) for kindly providing the cDNA used for the hERG Assay. We are also thankful for the excellent support by E. V. Dalietou, C. Dworschak, M. Guèrin, and A. Hodzic.

Supporting Information Available

Molecular Docking study, cytotoxic results, synthesis route for synthesis of **39** (Scheme S1), experimental procedures, and characterisation data for final compounds and intermediates **20a-64b** are reported in the Supporting Information.

References

(1) Robinson, M. C. An epidemic of virus disease in Southern Province, Tanganyika Territory, in 1952-53. I. Clinical features. *Transactions of The Royal Society of Tropical Medicine and Hygiene* **1955**, *49*, 28–32.

(2) Chretien, J. P.; Anyamba, A.; Bedno, S. A.; Breiman, R. F.; Sang, R.; Sergon, K.; Powers, A. M.; Onyango, C. O.; Small, J.; Tucker, C. J.; Linthicum, K. J. Drought-associated chikungunya emergence along coastal East Africa. *American Journal of Tropical Medicine and Hygiene* **2007**, *76*, 405–407.

(3) Vazeille, M.; Moutailler, S.; Coudrier, D.; Rousseaux, C.; Khun, H.; Huerre, M.; Thiria, J.; Bastien Dehecq, J.-S.; Fontenille, D.; Schuffenecker, I.; Despres, P.; Failloux, A.-B. Two Chikungunya isolates from the outbreak of La Reunion (Indian Ocean) exhibit different patterns of infection in the mosquito, Aedes albopictus. *PloS ONE* **2007**, *2*, e1168.

(4) Zeller, H.; Van Bortel, W.; Sudre, B. Chikungunya: Its History in Africa and Asia and Its Spread to New Regions in 2013-2014. *The Journal of Infectious Diseases* **2015**, *214*, 436–440.

(5) Venturi, G. et al. Detection of a chikungunya outbreak in central Italy, August to September 2017. *Eurosurveillance* **2017**, *22*, 11–14.

(6) Calba, C. et al. Preliminary report of an autochthonous chikungunya outbreak in France, July to September 2017. *Eurosurveillance* **2017**, *22*, 5–10.

(7) WHO Media Centre, Chikungunya - key facts. 2020; `https://www.who.int/news-room/fact-sheets/detail/chikungunya`, Acccessed: 31.05.2022.

(8) Campbell, L. P.; Luther, C.; Moo-Llanes, D.; Ramsey, J. M.; Danis-Lozano, R.; Peterson, A. T. Climate change influences on global distributions of dengue and chikungunya virus vectors. *Philos Trans R Soc Lond B Biol Sci* **2015**, *370*, 1–9.

(9) Thiberville, S.-D.; Moyen, N.; Dupuis-Maguiraga, L.; Nougairede, A.; Gould, E. A.; Roques, P.; De Lamballerie, X. Chikungunya fever: epidemiology, clinical syndrome, pathogenesis and therapy. *Antiviral Research* **2013**, *99*, 345–370.

(10) Ross, R. W. The Newala epidemic. III. The virus: isolation, pathogenic properties and relationship to the epidemic. *Journal of Hygiene* **1956**, *54*, 177–191.

(11) Borgherini, G.; Poubeau, P.; Jossaume, A.; Gouix, A.; Cotte, L.; Michault, A.; Arvin-Berod, C.; Paganin, F. Persistent arthralgia associated with chikungunya virus: a study of 88 adult patients on reunion island. *Clinical Infectious Diseases* **2008**, *47*, 469–475.

(12) Lebrun, G.; Chadda, K.; Reboux, A. H.; Martinet, O.; Gaüzère, B. A. Guillain-Barré Syndrome after Chikungunya Infection. *Emerging Infectious Diseases* **2009**, *15*, 495–496.

(13) Battisti, V.; Urban, E.; Langer, T. Antivirals against the Chikungunya Virus. *Viruses* **2021**, *13*, 1307.

(14) Kennedy Amaral Pereira, J.; Schoen, R. T. Management of chikungunya arthritis. *Clinical Rheumatology* **2017**, *36*, 2179–2186.

(15) Moesslacher, J.; Battisti, V.; Delang, L.; Neyts, J.; Abdelnabi, R.; Pürstinger, G.; Urban, E.; Langer, T. Identification of 2-(4-(Phenylsulfonyl)piperazine-1-yl)pyrimidine Analogues as Novel Inhibitors of Chikungunya Virus. *ACS Medicinal Chemistry Letters* **2020**, *11*, 906–912.

(16) Abdelnabi, R. et al. Novel Class of Chikungunya Virus Small Molecule Inhibitors That Targets the Viral Capping Machinery. *Antimicrobial Agents and Chemotherapy* **2020**, *64*, e00649–20.

(17) Moussa, I. A.; Banister, S. D.; Beinat, C.; Giboureau, N.; Reynolds, A. J.; Kassiou, M. Design, Synthesis, and Structure-Affinity Relationships of Regioisomeric N-Benzyl Alkyl Ether Piperazine Derivatives as σ-1 Receptor Ligands. *Journal of Medicinal Chemistry* **2010**, *53*, 6228–6239.

(18) Leonczak, P.; Srivastava, P.; Bande, O.; Schepers, G.; Lescrinier, E.; Herdewijn, P. N8-Glycosylated 8-Azapurine and Methylated Purine Nucleobases: Synthesis and Study of Base Pairing Properties. *Journal of Organic Chemistry* **2019**, *84*, 13394–13409.

(19) Wieder, O.; Kuenemann, M.; Wieder, M.; Seidel, T.; Meyer, C.; Bryant, S. D.; Langer, T. Improved Lipophilicity and Aqueous Solubility Prediction with Composite Graph Neural Networks. *Molecules* **2021**, *26*.

(20) Seley-Radtke, K. L.; Yates, M. K. The evolution of nucleoside analogue antivirals: A review for chemists and non-chemists. Part 1: Early structural modifications to the nucleoside scaffold. *Antiviral Research* **2018**, *154*, 66–86.

(21) Eyer, L.; Nencka, R.; de Clercq, E.; Seley-Radtke, K.; Růžek, D. Nucleoside analogs as a rich source of antiviral agents active against arthropod-borne flaviviruses. *Antiviral Chemistry and Chemotherapy* **2018**, *26*, 1–28.

(22) Delang, L. et al. The viral capping enzyme nsP1: a novel target for the inhibition of chikungunya virus infection. *Scientific Reports* **2016**, *6*, 31819.

(23) Kovacikova, K.; Morren, B. M.; Tas, A.; Albulescu, I. C.; Van Rijswijk, R.; Jarhad, D. B.; Shin, Y. S.; Jang, M. H.; Kim, G.; Lee, H. W.; Jeong, L. S.; Snijder, E. J.; Van Hemert, M. J. 6'-β-Fluoro-Homoaristeromycin and 6'-Fluoro-Homoneplanocin A

Are Potent Inhibitors of Chikungunya Virus Replication through Their Direct Effect on Viral Nonstructural Protein 1. *Antimicrobial Agents and Chemotherapy* **2020**, *64*, 02532–19.

(24) Mudgal, R.; Mahajan, S.; Tomar, S. Inhibition of Chikungunya virus by an adenosine analog targeting the SAM-dependent nsP1 methyltransferase. *FEBS Letters* **2020**, *594*, 678–694.

(25) Hiesinger, K.; Dar'In, D.; Proschak, E.; Krasavin, M. Spirocyclic Scaffolds in Medicinal Chemistry. *Journal of Medicinal Chemistry* **2021**, *64*, 150–183.

(26) Talele, T. T. Opportunities for Tapping into Three-Dimensional Chemical Space through a Quaternary Carbon. *Journal of Medicinal Chemistry* **2020**, *63*, 13291–13315.

(27) Wei, W.; Cherukupalli, S.; Jing, L.; Liu, X.; Zhan, P. Fsp^3: A new parameter for drug-likeness. *Drug Discovery Today* **2020**, *25*, 1839–1845.

(28) Lovering, F.; Bikker, J.; Humblet, C. Escape from flatland: Increasing saturation as an approach to improving clinical success. *Journal of Medicinal Chemistry* **2009**, *52*, 6752–6756.

(29) Bassetto, M.; Massarotti, A.; Coluccia, A.; Brancale, A. Structural biology in antiviral drug discovery. *Current Opinion in Pharmacology* **2016**, *30*, 116–130.

(30) Hughes, J.; Rees, S.; Kalindjian, S.; Philpott, K. Principles of early drug discovery. *British Journal of Pharmacology* **2011**, *162*, 1239–1249.

(31) Stork, C.; Embruch, G.; Šícho, M.; De Bruyn Kops, C.; Chen, Y.; Svozil, D.; Kirchmair, J. NERDD: a web portal providing access to in silico tools for drug discovery. *Bioinformatics* **2020**, *36*, 1291–1292.

(32) Šícho, M.; Stork, C.; Mazzolari, A.; De Bruyn Kops, C.; Pedretti, A.; Testa, B.; Vistoli, G.; Svozil, D.; Kirchmair, J. FAME 3: Predicting the Sites of Metabolism in Synthetic Compounds and Natural Products for Phase 1 and Phase 2 Metabolic Enzymes. *Journal of Chemical Information and Modeling* **2019**, *59*, 3400–3412.

(33) Penning, T. D. et al. Synthesis and biological evaluation of the 1,5-diarylpyrazole class of cyclooxygenase-2 inhibitors: identification of 4-[5-(4-methylphenyl)-3-(trifluoromethyl)-1H-pyrazol-1-yl]benze nesulfonamide (SC-58635, celecoxib). *Journal of Medicinal Chemistry* **1997**, *40*, 1347–1365.

(34) Clader, J. W. The Discovery of Ezetimibe: A View from Outside the Receptor. *Journal of Medicinal Chemistry* **2004**, *47*, 1–9.

(35) Johnson, B. M.; Shu, Y.-Z.; Zhuo, X.; Meanwell, N. A. Metabolic and Pharmaceutical Aspects of Fluorinated Compounds. *Journal of Medicinal Chemistry* **2020**, *63*, 6315–6386.

(36) Purser, S.; Moore, P. R.; Swallow, S.; Gouverneur, V. Fluorine in medicinal chemistry. *Chemical Society Reviews* **2008**, *37*, 320–330.

(37) Chaitanya, G. V.; Alexander, J. S.; Babu, P. P. PARP-1 cleavage fragments: Signatures of cell-death proteases in neurodegeneration. *Cell Communication and Signaling* **2010**, *8*, 31.

(38) Wolber, G.; Langer, T. LigandScout: 3-D pharmacophores derived from protein-bound ligands and their use as virtual screening filters. *Journal of Chemical Information and Modeling* **2005**, *45*, 160–169.

(39) Baburin, I.; Beyl, S.; Hering, S. Automated fast perfusion of Xenopus oocytes for drug screening. *Pflugers Archiv European Journal of Physiology* **2006**, *453*, 117–123.

(40) Kratz, J. M.; Schuster, D.; Edtbauer, M.; Saxena, P.; Mair, C. E.; Kirchebner, J.; Matuszczak, B.; Baburin, I.; Hering, S.; Rollinger, J. M. Experimentally validated hERG pharmacophore models as cardiotoxicity prediction tools. *Journal of Chemical Information and Modeling* **2014**, *54*, 2887–2901.

(41) Berthold, M. R.; Cebron, N.; Dill, F.; Gabriel, T. R.; Kötter, T.; Meinl, T.; Ohl, P.; Sieb, C.; Thiel, K.; Wiswedel, B. In *Data Analysis, Machine Learning and Applications*; Preisach, C., Burkhardt, H., Schmidt-Thieme, L., Decke, R., Eds.; Springer: New York, 2008.

(42) Stork, D.; Timin, E. N.; Berjukow, S.; Huber, C.; Hohaus, A.; Auer, M.; Hering, S. State dependent dissociation of HERG channel inhibitors. *British Journal of Pharmacology* **2007**, *151*, 1368–1376.

(43) Shabbir, W.; Topcagic, N.; Aufy, M. Activation of autosomal recessive Pseudohypoaldosteronism1 ENaC with aldosterone. *European Journal of Pharmacology* **2021**, *901*, 174090.

(44) Willam, A.; Aufy, M.; Tzotzos, S.; Evanzin, H.; Chytracek, S.; Geppert, S.; Fischer, B.; Fischer, H.; Pietschmann, H.; Czikora, I.; Lucas, R.; Lemmens-Gruber, R.; Shabbir, W. Restoration of epithelial sodium channel function by synthetic peptides in pseudohypoaldosteronism type 1B mutants. *Frontiers in Pharmacology* **2017**, *8*, 85.

(45) Shabbir, W.; Topcagic, N.; Aufy, M.; Oz, M. CRISPR/CAS9 mediated knock down of δ-ENaC blunted the TNF-induced activation of ENaC in A549 cells. *International Journal of Molecular Sciences* **2021**, *22*, 1–10.

(46) Willam, A. et al. TNF lectin-like domain restores epithelial sodium channel function in frameshift mutants associated with pseudohypoaldosteronism type 1B. *Frontiers in Immunology* **2017**, *8*, 601.

TOC Graphic

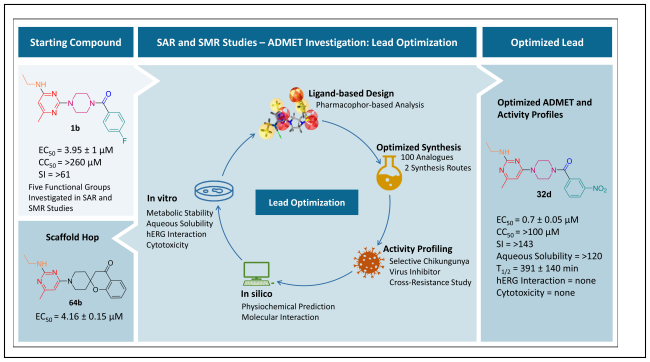
Starting Compound
SAR and SMR Studies – ADMET Investigation: Lead Optimization
Optimized Lead
1b
EC50 = 3.95 ± 1 µM
CC50 = >260 µM
SI = >61
Five Functional Groups Investigated in SAR and SMR Studies
Scaffold Hop
64b
EC50 = 4.16 ± 0.15 µM
Ligand-based Design
Pharmacophor-based Analysis
Optimized Synthesis
100 Analogues
2 Synthesis Routes
Activity Profiling
Selective Chikungunya Virus Inhibitor
Cross-Resistance Study
In silico
Physiochemical Prediction
Molecular Interaction
In vitro
Metabolic Stability
Aqueous Solubility
hERG Interaction
Cytotoxicity
Lead Optimization
Optimized ADMET and Activity Profiles
32d
EC50 = 0.7 ± 0.05 µM
CC50 = >100 µM
SI = >143
Aqueous Solubility = >120
T1/2 = 391 ± 140 min
hERG Interaction = none
Cytotoxicity = none